



Student Name Patrick Morrison Student ID \*\*\*\*\*

Master's          Degree in Ecology and Evolutionary Biology

Thesis Title:

Tracing the early emergence of microbial sulfur metabolisms

Have you performed research involving human subjects which requires approval from the Institutional Review Board (IRB)?  Yes  No

IRB Protocol Number                                 

Have you used live animals, animal tissue, or observational animal work which requires approval from the Institutional Animal Care and Use Committee (IACUC)?  Yes  No

IACUC Protocol Number                                 

Attach the final copy of thesis/dissertation for committee review. While formatting changes may be requested by the Graduate School, the content of the attached document should be final.



**Approvals:**

Committee Chair Name William Adams

Signature  Date Signed 12/1/2020

Committee Member Name Samuel Flaxman

Signature  Date Signed 12/1/2020

The final copy of this thesis has been examined by the signatories, and we find that both the content and the form meet acceptable presentation standards of scholarly work in the above-mentioned discipline.

# **Tracing the early emergence of microbial sulfur metabolisms**

By

**Patrick R. Morrison**

B.S., Northern Illinois University

Department of Biological Sciences., 2013

This thesis is submitted for review to  
The faculty of the graduate school of the  
University of Colorado, Boulder in the  
Partial fulfillment of the requirements  
For the degree of a Masters of Arts  
By the department of  
Ecology and Evolutionary Biology 2020

This thesis entitled:  
Tracing the early emergence of microbial sulfur metabolisms  
written by Patrick R. Morrison  
has been approved for the Department of Ecology and Evolutionary Biology

---

Stephen J. Mojzsis



---

William W. Adams III



---

Samuel M. Flaxman

Date \_\_\_\_\_

The final copy of this thesis has been examined by the signatories, and we find that both the content and the form meet acceptable presentation standards of scholarly work in the above-mentioned discipline.

Patrick Morrison (M.S., Ecology and Evolutionary Biology)

Tracing the Early Emergence of Microbial Sulfur Metabolisms

Thesis directed by Professor Stephen Mojzsis

Hydrogen sulfide ( $n\text{H}_2\text{S}$ ) and sulfur oxide ( $\text{SO}_n$ ;  $n=1,2,3$ ) gases in early Earth's globally anoxic atmosphere were subjected to gas-phase chemical transformations by ultraviolet light. A principal photolysis pathway at that time produced elemental sulfur aerosols with mass-independently fractionated (MIF) isotopic values carrying variable minor isotope compositions ( $^{33}\text{S}$ ,  $^{36}\text{S}$ ). These rained into the sulfate-deficient Archean (ca. 3.85-2.5 giga-annum [Ga], or billions of years ago) oceans to react with  $[\text{Fe}^{2+}]_{\text{aq}}$  and form sedimentary sulfides. The MIF-bearing sulfides were incorporated into Archean sediments, including banded iron-formations (BIF). Such aerosols may also have fueled microbial sulfur metabolisms, and thus are traceable by the MIF sulfur isotopes. Yet, data show that before  $\sim 3.5$  Ga *mass-dependent*  $^{34}\text{S}/^{32}\text{S}$  values in Early Archean sediments tend to fall within a narrow ( $\pm 0.1\%$ ) range even as they carry *mass-independent* values. By about 3.5 Ga,  $^{34}\text{S}/^{32}\text{S}$  values show much greater changes ( $>1\%$ ) in range congruent with microbial metabolic processing. Here, I trace probable pathways of elemental sulfur aerosols into Archean sediments, and couple my study with analysis of the evolutionary relationships of enzymes involved in sulfur metabolism to explain the observed trends. The narrative proposed is that while an immediate

precursor to the enzyme required to metabolize  $S^0$  was present prior to 3.5 Ga, at this point, sulfur reduction was e- donor limited due to high ratios of oxidized sulfur compounds to molecular hydrogen in volcanic vents. What distinguished the biosphere after 3.5 Ga was the advent of (and if not the rapid expansion of brought on by P fertilization of the oceans) of photosynthesis which given the high ratio of sulfides to sulfate in hydrothermal vents, would have produced an excess of electron donors in the form of organic carbon. The removal of sulfate as barite in the periphery of the vent communities would induce a situation where sulfur reduction was electron acceptor limited thus driving contemporary organisms to utilize another form of sulfur (in this case, photolytically produced elemental sulfur aerosols). This model explains why elemental sulfur aerosols were apparently not utilized by the Eoarchean (pre-3.65 Ga) biosphere even though an immediate precursor to the required enzyme may have already been present.

## **Acknowledgements**

I would like to acknowledge the support that my family has provided for me throughout my time at the University of Colorado. My parents (Debra Beres and Timothy Morrison) have helped nurture my scientific curiosity from a young age and find my calling in life. I also know that I can count on their support wherever life takes me after my time in graduate school. I would also like to acknowledge the love, company and emotional support that my two cockatiels Mocha and Frieda have provided to me.

**Table of Contents:**

<b>Chapter 1</b>	Introduction.....	1
1.1	<i>Sulfur Isotope geochemistry as a tracer of ancient environments and metabolisms</i> .....	2
1.2	<i>Antiquity of Acetyl-CoA and its relationship to alkaline hydrothermal vents</i> .....	4
1.3	<i>Enzymes involved in dissimilatory Sulfur reduction</i> .....	8
<b>Chapter 2</b>	<b>Data Acquisition and Analysis</b> .....	9
2.1	<i>Data Acquisition</i> .....	9
2.2	<i>Source Data Geologic Setting</i> .....	10
2.3	<i>Source S-Isotope Measurements</i> .....	12
<b>Chapter 3</b>	Reporting multiple sulfur isotope heterogeneities in the geologic record.....	14
3.1	<i>Conventional notations for the multiple sulfur isotopes</i> .....	14
3.2	<i>MDF and MIF fractionation processes documented in the Archean sulfur cycle</i> .....	17
3.2.1	<i>Atmospheric photochemistry and multiple sulfur isotopes</i> .....	17
3.2.2	<i>Archean MIF sulfur aerosols, atmosphere transparency, low pO<sub>2</sub>, and scattering</i> .....	21
3.2.3	<i>Using polar coordinates to interpret multiple S-isotope data</i> .....	22
3.3	<i>Archean sulfur metabolisms</i> .....	25
3.3.1	<i>Mineralogical aspects of microbial “sulfate reduction”</i> .....	25
3.3.2	<i>Mineralogical aspects of microbial sulfur disproportionation</i> .....	28
3.3.3	<i>Post-depositional abiotic sulfur isotope fractionation processes</i> .....	29
3.4	<i>Microbial sulfur reduction in the Archean marine system</i> .....	30
3.4.1	<i>Authigenic sulfide mineral formation in Archean banded iron-formations</i> .....	31
3.4.2	<i>Secular <math>\delta^{34}\text{S}</math> trends in Eoarchean-Paleoarchean sulfides</i> .....	32
<b>Chapter 4</b>	Evolution of biological sulfur cycling on the Eoarchean to Paleoarchean Earth.....	35
4.1	<i>Eoarchean alkaline hydrothermal vents as a waystation for early life</i> .....	35
4.2	<i>Environmental availability of free hydrogen</i> .....	37
4.3	<i>Selective pressures on the early biochemical evolution of sulfur metabolism</i> .....	38
4.3.1	<i>Sulfite detoxification</i> .....	39
4.4.2	<i>Rise of sulfate, thiosulfate, tetrathionate and elemental sulfur metabolisms</i> .....	42

4.4.3 Arrival of photolithotrophy.....	44
<b>Chapter 5 Discussion.....</b>	<b>45</b>
5.1 Straying from the alkaline vent.....	45
5.2 Sulfur and the dawn of photolithotrophy.....	47
5.3 Elemental sulfur reduction appears in the Paleoarchean as opposed to other $S^0$ pathway....	49
5.4 The phosphorus connection and an age-old question of evolutionary biology.....	51
5.5 A mesoarchean “iron age” of metabolism.....	54
<b>Chapter 5 Conclusions.....</b>	<b>59</b>
References.....	66



**List of figures:**

Figure 1. Schematic diagram of the sedimentary sulfur cycle.....5

Figure 2. The major dissimilatory sulfur reduction pathways.....13

Figure 3. The multiple sulfur isotope record of the different stages of the Archean..... 18

Figure 4. Polar coordinate plot of Eo-Mesoarchean MIF sulfur isotope record.....25

Figure 5. Schematic diagram of inorganic sulfur redox reactions in the marine system.....27

Figure 6. Position of the DsrA and DsrB subunits within the phylogeny of Dsr-like proteins.....41

Figure 7. A proposed scenario for the evolution of the *Phs* and *Psr/Sre* enzymes.....45

Figure 8. Concentrations of phosphorus by percent weight from Archean carbonate sediments.....53

Figure 9. Possible phylogeny of the photosystems used in photosynthesis.....56

## Chapter 1. Introduction

Earth's biosphere is ancient, its origin evidently pre-dates the geologic record (Benner et al. 2020). Although the various lines of evidence for life's antiquity are debated, the fixation of organic carbon by biological activity from the earliest times is tentatively attested by the presence of  $^{13}\text{C}$ -depleted carbonaceous matter captured within rocks of marine sedimentary origin dated to be about 3.8 giga annum (Ga; or billions of years ago); low  $^{13}\text{C}/^{12}\text{C}$  carbonaceous matter is a characteristic isotopic feature of metabolic activity associated with carbon fixation (Schidlowski, 1988; Mojzsis et al. 1996; Rosing 1999; cf. Whitehouse et al. 2009). Other evidence, also strongly contested, for relatively sophisticated microbial communities before ca. 3.7 Ga include purported "stromatolite-like" microfossil shapes from ca. 3.71 Ga rocks in the Isua supracrustal belt of West Greenland (Nutman et al. 2016; cf. Allwood et al. 2018; Zawaski et al. 2020) and alleged "microfossils" found within hydrothermal jaspilites of the ca. 3.78 Ga Nuvvuagittuq locality in Canada (Dodd et al. 2015; cf. Greer et al. 2020). Yet older and similarly strongly disputed hints of life are offered by  $^{12}\text{C}$ -enriched graphite within rocks from the Nulliak assemblage in Labrador, Canada, that are suspected to be as old as ca. 3.95 Ga (Tashiro et al. 2019; cf. Whitehouse et al. 2019). Lastly, a few ca. 4.1 Ga zircons host inclusions of  $^{12}\text{C}$ -enriched amorphous carbon (as hexagonal pseudomorphs after graphite) that offer the tantalizing prospect of an emergent Hadean biome (Bell et al. 2015; cf. Alleon and Summons 2019). Beyond these uncertain fossil traces from a patchy geological record, however, we have little direct knowledge of the operative metabolic style(s) that were present in the biosphere's first billion years. As it stands, there appears to have been a biosphere present on Earth

by about 4 billion years ago that had the ability to fix organic carbon from inorganic sources. What was the nature of this microbial biosphere, and how could it have manifested itself in other ways?

### *1.1 Sulfur isotope geochemistry as a tracer of ancient environments and metabolisms*

The many geomicrobiological insights provided by sulfur ultimately emanate from variations in its 8 (-II to +VI) valence states (**Figure 1**). This is reflected in a rich metal-sulfur chemistry and mineralogy, as well as the isotopic composition in sulfur-containing minerals found in sedimentary rocks. These variations reflect the different partitioning of its four stable isotopes into various compounds via certain biochemical reactions under different environmental regimes. Technically, such induced variation is termed “stable isotope fractionation”. Specific biochemical reactions associated with different microbial metabolic styles can thus produce compounds with characteristic sulfur isotopic ratios that are interpretable if the source isotopic composition and reaction pathways are known (or inferred). In this way, it becomes possible to use the isotopic compositions of sedimentary sulfur minerals to pinpoint metabolic styles in the geologic record. The approach to using sulfur isotopes in this way has a long history (e.g., Monster et al. 1979; Schidlowski et al. 1983; Strauss 1993, 1997, 2003). As reviewed elsewhere (e.g., Mojzsis 2007) surface geochemical cycling of sulfur from the beginning of the continuous geologic record at ca. 3.85 Ga (Nutman et al. 1997) to the rise of atmospheric oxygen around 2.42 Ga (Papineau et al. 2007) is understood to have been dominated by atmospheric reactions under neutral and anoxic conditions (Farquhar et al. 2000, 2001; Pavlov and Kasting 2002). These UV-generated gas phase reactions (**Chapter 3.2.1**) produced sulfur compounds with anomalous

enrichments and depletions in the minor sulfur isotopes ( $^{33}\text{S}$ ,  $^{36}\text{S}$ ) and can be preserved in the rock record (e.g., Farquhar and Wing 2003).

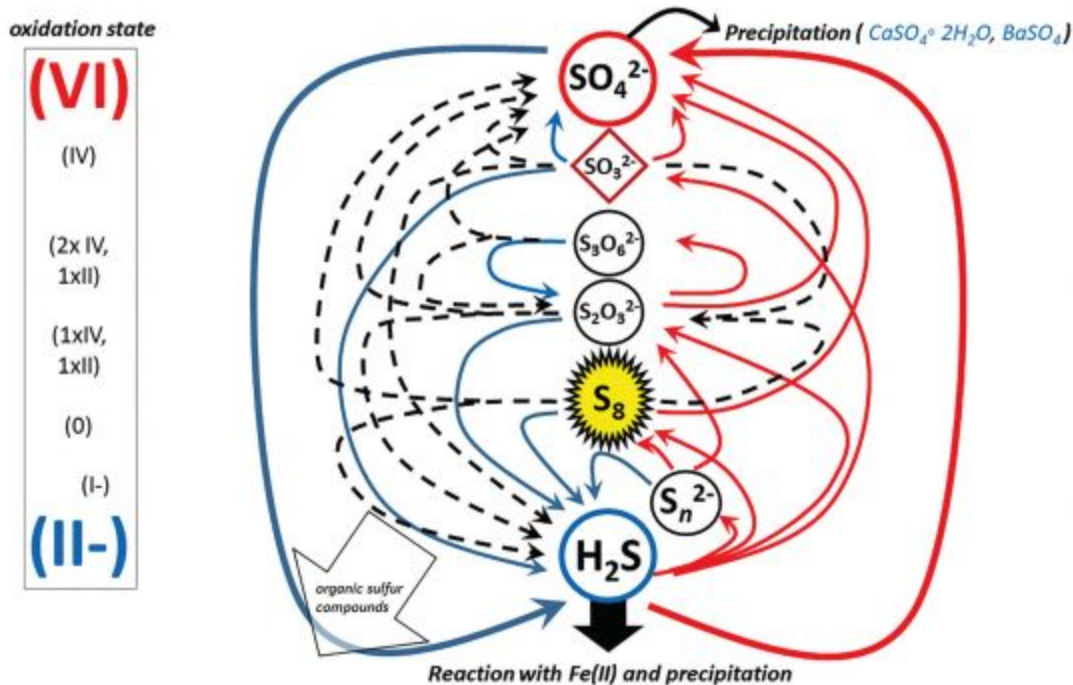


Figure 1. Schematic diagram of the sedimentary sulfur cycle with reductive (blue line at left, downward arrows) and oxidative (red line at right, upward arrows) pathways illustrated with respect to valence state (II to p VI). Dashed lines in the reductive regime (LEFT) represent microbial disproportionation reactions. In this representation, the sulfur cycle is powered either by degradation of organic matter via sulfate-reducers (heavy blue arrow), or sulfide oxidation (heavy red arrow), or intermediate pathways such as elemental sulfur (aerosol;  $\text{S}_8$  reduction/oxidation). Sedimentation and burial of ferrous-sulfide minerals (mostly  $\text{FeS}_2$ ; but see Figure 3 that includes intermediate mackinawite and greigite) is the dominant sink for reduced sulfur in the marine sedimentary system (modified after Zopf et al. 2004).

Long-term variations in these sulfur isotope signatures and the timing of their appearance (and *disappearance*) from the geologic record are now routinely used to analyze atmospheric chemical changes over geologic timescales and, important for this work, the early evolution of the surface zone up to the Paleoproterozoic era (2.5-1.6 Ga; e.g., Kumar and Francisco 2017). In particular, the last two decades have focused on using this powerful multifarious sulfur isotopic tool (MDF/MIF) to determine the timing of

the irreversible oxygenation of the surface zone at the Great Oxidation Event at ca. 2.42 Ga (Holland 2006; Papineau et al. 2007; Kaufman et al. 2007).

A less-exploited component of the Earth's early sulfur cycle is to study how observed changes in both the magnitude of anomalous minor isotope ( $^{33}\text{S}$ ) enrichments and depletions, along with changes in the absolute ranges of  $^{34}\text{S}/^{32}\text{S}$ , relate to metabolic innovations that appeared at different times owing to changes in local as well as global selection pressures. The review by Thiemens and Lin (2019) provides the appropriate background information of this chemistry to begin to make sense of how we can trace the emergence of life with this interesting chemistry.

Here, I direct my attention to the multiple sulfur isotope geochemistry for which data exist for the world's oldest sediments – mostly comprised of the BIFs – followed by an overview of the isotopic fractionation processes believed to be involved in the Archean biosphere. Furthermore, I explain how the sulfur isotopic signatures produced by these processes can be used as tracers of the pathways by which elemental sulfur reached the microbial biosphere and to follow its subsequent modifications. A peculiar trend that is observed in the geologic record is that during the Eoarchean period,  $\delta^{34}\text{S}$  values seldom deviate from the Archean reference array (ARA) by more than 5‰ while in the Paleoarchean, many sulfides have  $\delta^{34}\text{S}$  values less than 10‰ (most of which have greater than 0‰  $\Delta^{33}\text{S}$  values) (Mojzsis, 2007). The implication of this is that during the Eoarchean, sulfur was not being metabolized in any detectable quantity while in the Paleoarchean, microbial sulfur reduction (MSR) was very abundant and the preferred source was elemental sulfur (Philippot et al 2007). The presence of  $\Delta^{33}\text{S}$  values greater than 0‰ prior to 3.5 indicates that, as in the Paleoarchean, UV

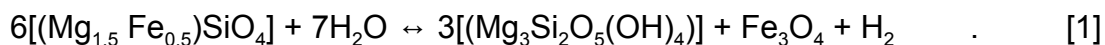
photolysis was producing elemental sulfur aerosols in the Eoarchean but the lack of deviation from the ARA indicates that said aerosols were not being used at the time. This begs a major question: what changed between the Eoarchean and Paleoarchean to cause the ancient biosphere to utilize elemental sulfur? Here, I use a combination of the evidence obtained from the geologic record along with comparative biochemistry of ancient metabolisms to make sense of the observed trends.

### *1.2 Antiquity of Acetyl-CoA and its relationship to alkaline hydrothermal vents*

One of the metabolisms most frequently argued to have been present very early in the history of life is the reductive acetyl-coenzyme A (Acetyl-CoA), or Wood-Ljungdahl (W-L) pathway (e.g. Ragsdale and Pearce 2008; Braakman and Smith 2012). The autotrophic Acetyl-CoA pathway uses free hydrogen from the environment as an electron donor and carbon dioxide as an electron acceptor. The last universal common ancestors of all extant life (dubbed LUCA) are thought to have comprised a population that used this Wood-Ljungdahl pathway in a primordial H<sub>2</sub>-powered biosphere, perhaps associated with hydrogenous alkaline hydrothermal settings (e.g., Weiss et al. 2016). I return to this setting later in my analysis. Meanwhile, it is important to note that the LUCA organism(s) had already reached a level of complexity that places them far from the origin of life, perhaps in the late Hadean. Further, going beyond the debate over whether or not life actually originated in hydrothermal vents on the seafloor or, alternatively, in shallow settings on dry land, evidence from molecular phylogenies points to hydrothermal vents as at least a waystation in early life's history from its origins to the crystallization of the genome that preceded Bacteria, Archaea and Eukarya (Pace 2006).

Still, a strong argument for at least a *syn*- or perhaps even *pre*-biotic origin of the Acetyl-CoA pathway comes from experiments that show native transition metals ( $\text{Fe}^0$ ,  $\text{Ni}^0$ ,  $\text{Co}^0$ ) can, under natural conditions, selectively reduce  $\text{CO}_2$  to  $\text{CH}_3\text{CO}_2^-$  and  $\text{C}_3\text{H}_4\text{O}_3$  (acetate and pyruvate, respectively; Varma et al. 2018). More recently, Preiner et al. (2020) showed that acetate and pyruvate are also formed under alkaline hydrothermal conditions from  $\text{H}_2$  and  $\text{CO}_2$  – as in the biological pathway – using only mixed-valence  $\text{Fe}(\pm\text{Ni})$ -oxides in water as the catalyst. Analysis also suggests that these ancient intermediates and end-product compounds of W-L pre-date LUCA (e.g., Goldford et al. 2019).

Native metals and alloys (e.g.,  $\text{Ni}_{2,3}\text{Fe}$ ; awaruite) are well known as mineralogical products of serpentinized peridotite within hydrothermal systems (Sousa et al. 2018). Furthermore, certain minerals of the Osmiridium-group (Os-Ir-Ru-Pt alloys) occur in serpentinized ultramafic rocks and their weathering detritus (e.g., Hattori and Cabri 1992). Briefly, serpentinization is the hydration of (peridotitic) olivine  $(\text{Mg},\text{Fe})_2\text{SiO}_4$  and orthopyroxene  $(\text{Mg},\text{Fe},\text{Ca}) (\text{Mg},\text{Fe},\text{Al}) (\text{Si},\text{Al})_2\text{O}_6$ . A general form of the serpentinization reaction involves the hydration reaction of olivine to form serpentine, magnetite and free hydrogen:



Significantly, these reactions exist wherever hot ultramafic rocks are in contact with water; they provide a reducing environment with high  $\text{H}_2$  concentrations where native metals catalyze hydrocarbon production with  $\text{H}_2$  as the electron donor (e.g., Proskurowski et al. 2008). I view this as a compelling natural chemical reactor space

that provides a prebiotic route to the origin of the W-L pathway and comports with the logical arguments provided in Russell and Martin (2004).

Aside from serving as a cradle for the early biosphere, widespread hydrothermal emanations from the extensive hot Archean seafloor crust dictated to no small degree the composition of early Earth's seawater. For example, rare earth element studies show that the plentiful  $\text{Fe}^{2+}$  present in the Archean (3.85 to 2.5 Ga) originated primarily from expulsion of metalliferous hydrothermal vent fluids (Jacobsen and Pimentel-Close 1988).

Taken together, it is unmistakable that the widespread hydrothermal environments on the primordial Earth provided a ready supply of native metals, simple organic molecules, and free hydrogen to power one of the stepping stones in the history of early life from its origin (someplace) to ultimate colonization of the global ocean. We posit that – at the least – an intermediate stage of life must have included residence around hydrothermal vents, that the vents were the primary sources of reactive iron (II) to account for the deposition of the ubiquitous banded iron-formations (e.g., Posth et al. 2013; **Chapter 3.3.1**), and that the combined geochemistry of the sulfur isotopes in the oldest known sediments and phylo-metabolic data is a testimony to this history.

Apart from carbon isotope studies of the oldest rock of sedimentary origins cited above, fractionations in the relative isotopic abundances of the other principal biophilic elements (Fe, N, and S; e.g., Thomazo et al. 2009 *and references therein*) are widely used to imply that a globally active biosphere was present in the first billion years. Among these, the stable isotopes of sulfur ( $^{32}\text{S}$ ,  $^{33}\text{S}$ ,  $^{34}\text{S}$ ,  $^{36}\text{S}$ ) stand out as a versatile



tool for the elucidation of oxidation modes and the metabolic styles of microbial communities in deep time (e.g., Johnston 2011).

### 1.3 *Enzymes involved in dissimilatory sulfur metabolism*

In the contemporary oceans MSR is responsible for ~50% of the remineralization of all organic matter (Grein et al. 2013). In this pathway (**Chapter. 3.2.1**), sulfate is taken up and reacts with ATP via sulfate adenylate transferase (*Sat*) to form APS (**Figure 2**). Then, an adenyl-sulfate reductase (*Apr*) enzyme cleaves the bond between the phosphate and sulfate group to form sulfite. This is then reduced to sulfide via a dissimilatory sulfite reductase (*Dsr*) located at the end of an electron transport chain; the electrons either being derived from an organic molecule or hydrogen (Grein et al. 2013). The enzymes that carry out the reactions are homologs, even if there are many alternative pathways oxidation usually takes (Weissgerber et al. 2014). Other forms of sulfur can also be utilized.

Elemental sulfur ( $S^0$ ), thiosulfate ( $S_2O_3^{2-}$ ), and tetrathionate ( $S_4O_6^{2-}$ ) can ultimately be reduced to sulfide via polysulfide/sulfur (*Psr/Sre*), thiosulfate (*Phs*) and tetrathionate (*Ttr*) reductases in sulfur reducing microbes (Laska et al. 2003). *Phs* reduces Thiosulfate to sulfite which is then reduced to sulfide via *Dsr* and tetrathionate is reduced to thiosulfate by *Ttr* which is then metabolized by *Phs* in the manner described. Meanwhile, *Psr* reduces polysulfides by reducing a sulfur atom at the end of a polysulfide to a monosulfide (Rabus et al. 2013). These enzymes are closely related to one another belonging to the molybdopterin oxidoreductase enzyme family (Duval et al. 2008).

While the sulfur oxidation and fermentation pathways are distinct metabolic pathways, there are some enzymes shared between the processes. Specifically, the *Dsr*, *Apr* and *Sat* enzymes are used to oxidize sulfide to sulfate (although unlike in sulfur reduction, there is an elemental sulfur intermediate). In contrast, elemental sulfur, thiosulfate and tetrathionate are oxidized to sulfate using *Sox* enzymes which belong in the cytochrome oxidase gene families (**Figure 2**). Furthermore, sulfides can be oxidized to elemental sulfur in sulfur oxidizers via sulfide quinone reductases (Gregersen et al. 2011). Finally, elemental sulfur and thiosulfate can be disproportionated (fermented) to produce sulfate and sulfide via sulfur oxidoreductases (Thamdrup et al. 1993).

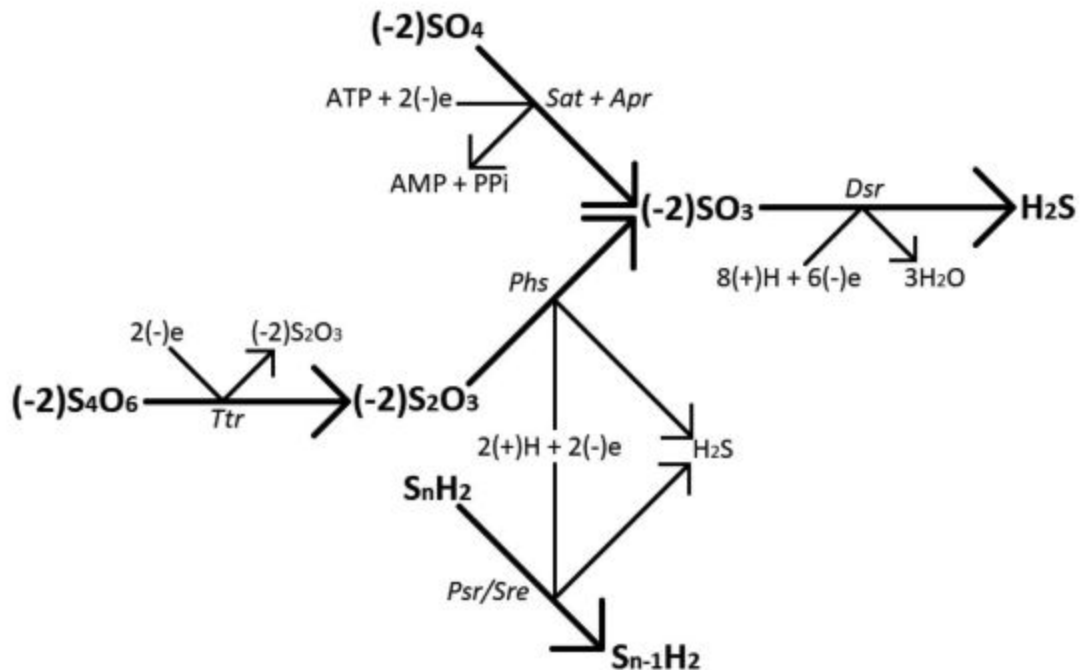


Figure 2. The major dissimilatory sulfur reduction pathways (modified from Rabus et al. 2013).

## Chapter 2. Data acquisition and analysis

### 2.1 Data Acquisition

The data presented here is a multiple sulfur isotope meta analysis. Such studies investigating the nature of the Archean Biosphere have used similar approaches before (Thomazo et al. 2009; Havig et al. 2017; Mojzsis et al. 2007). Here, multiple publications were collected and the data were obtained and put into excel spreadsheets. The data included in the spreadsheet were the age of the sample, the source location, the source mineral, and the method by which the sulfur isotope was measured. The samples were then organized by age in 100 mega annum (Ma) intervals spanning the course of the Archean Eon. To synthesize the data used for Figure 3, all of the points for which  $\Delta^{33}\text{S}$  and  $\delta^{34}\text{S}$  values were available from each of the four eras of the Archean (Eo, Paleo, Meso, and Neo) was catenated and plotted with the mass independent fractionation on the Y-axis and the mass dependent fractionation on the X-axis. To obtain a better understanding of the patterns of UV photolysis that occurred over the course of the Archean, samples for which the  $\Delta^{33}\text{S}$  and  $\Delta^{36}\text{S}$  values were available had the hypotenuse of the mass independent fractionation ( $\Delta^{33}\text{S}$  and  $\Delta^{36}\text{S}$ ) calculated as well as the array slope to serve as proxies for the degree of mass independent fractionation and the wavelength the sample was subjected to respectively (for more information, see **Chapter 3.2.3**). To visually represent the data, the age was represented by the X-axis, the angle by the Y-axis, and the degree of mass independent fractionation as the 'Z-axis' in the form of a color bar. A similar, albeit more simplified, approach was used for the phosphorus record throughout the Archean. Phosphorus percent weight data from carbonates over the course of the Archean were obtained

along with information about the age and the location of the sample, all of which were entered in an excel sheet. For both sulfur isotope and phosphorus constituency data, sources for each data point were numbered and the corresponding number was stored in a separate document. A link to the github is at the bottom of this document.

## *2.2 Source Data Geologic Setting*

Although the data from samples spanning across the Archean were reported in this data set, given that the main focus of this dissertation was the difference observed between the Paleoarchean and Eoarchean, most of the samples came from one of three sites. The oldest is the Isua formation (dating from the Eoarchean) in southwestern Greenland and a few surrounding locations (Polat et al. 2003). The second oldest is the Dresser Formation in northwestern Australia (dated from the early to mid-Paleoarchean); it is in these rocks that the widespread utilization of  $S^0$  by sulfur reducing microbes is attested (Van Kranendock et al. 2008). The third area is the Barberton formation of southern Africa where most formations are dated from the late Paleoarchean even though some sites date to prior to the Dresser formation (Gutzmer et al. 2006).

The Canadian shield has yielded the most ancient rocks on the contemporary Earth such as the 4 Ga “Acasta Gneiss” (Stern et al. 1998). On the shores of the North Atlantic and Arctic oceans, the remains of the oldest attested habitats can be found in the Isua, Akilia (Greenland), and Nuuvutuq (Canada) formations (O’Neil et al. 2012). The most extensively studied of these formations is Isua, an ancient greenstone belt dated to between 3742 and 3710 Ma (Polat et al. 2003). This formation is primarily composed of gneiss with intermittent banded iron formations (but these are primarily

composed of magnetite and are of the algonia-type variety while the more famous ones from the Neoproterozoic are composed primarily of hematite and are of the “superior” variety) and amphibolites. These belts are of the “metasedimentary” and “metavolcanic”, or partially metamorphosed sedimentary and volcanic rocks respectively (Bolhar et al. 2005). Another, somewhat older site from southwestern Greenland is the Akilia site dated from 3883 Ma but this site has been subjected to a greater degree of diagenesis (Lepland and Whitehouse, 2011). The third major ancient formation from the Canadian Shield is Nuvvuaittuq. Like Isua and Akilia, this formation is composed primarily of greenstone but the date is unresolved with some estimates giving an age of 3750 Ma and another dating it back to the Hadean (4338 Ma) (O’neil et al. 2012). Given the age of formation, the Isua, Akilia and Nuvvuagittuq sites can give invaluable insight into the environments present on the Earth less than 1 Ga after the moon forming impact (Bottke et al. 2015).

The Dresser Formation is part of the Warrawoona group located in the Pilbara Craton (Van Kranendock et al. 2008). A nearby site that has also yielded evidence of early biological activity is the Stelley pool formation and the maximum age estimate for these formations is approximately 3490 Ma (Van Kranendock et al. 2008). These formations consist primarily of basaltic greenstones with intermittent cherts (Van Kranendock et al. 2008). A series of silica veins occurring between faults appear to have been of hydrothermal origin and have also contributed to the sedimentary environment (Van Kranendock et al. 2008). Within the chert layers and veins, intermittent barite deposits with pyrite nodules are present (Van Kranendock et al. 2008).

The third major location that has yielded many samples for this meta-analysis is the Barberton Greenstone Belt. While most of the rocks within this belt are of igneous origin, there is still a plentiful supply of Paleoproterozoic sedimentary deposits (Van Kranendonk et al. 2009). This belt was laid down over a period of around 500 Ma with the Theespruit formation being the oldest at 3548 Ma (Van Kranendonk et al. 2009). Another formation within the Barberton supergroup is known as the “Buck Reef Chert” that has been dated to 3416 Ma. This formation is composed of carbonaceous and ferruginous cherts overlaying a slightly older layer of volcanoclastic rocks (Ledevine et al. 2019). Due to the similarity in age between the Buck Reef Chert and the aforementioned Dresser Formation, comparing these two sites can provide insight into how “global” perturbations to the biosphere and sulfur cycle 3.5 Ga were. One of the more prominent formations in the Barberton Greenstone Belt is the Mapepe Formation dated to between 3259 and 3226 Ma (Gutzmer et al. 2006). This layer is composed primarily of terrigenous sedimentary rocks interbedded with volcanoclastic rocks (Gutzmer et al. 2006).

### *2.3 Source S-Isotope Measurements*

In order to determine the sulfur isotope composition of the Archean sediments, a number of techniques were employed. The most preferred method is known as Inductively Coupled Plasma Ion Mass Spectrometry (Craddock et al. 2008). This analysis method uses an electrically charged gas to ionize the atoms in a sample (Craddock et al. 2008). These ions are then accelerated and passed through a magnetic field (Craddock et al. 2008). Due to the lower mass to charge ratio of the lighter isotopes, such atoms will undergo a greater degree of trajectory alteration and

will thus flow into different collection chambers than the heavier isotopes, allowing for the isotopic composition of a given sample to be determined (Craddock et al. 2008). Other methods include gas source mass spectrometry that, in the case of these samples, involved “burning” the sulfur into  $\text{SO}_2$ , ionizing it, and measuring the deflection. A problem with this approach is the variable weight of oxygen isotopes that can make a sulfur dioxide molecule heavier than most isotopologues while containing the most abundant mass sulfur ( $^{32}\text{S}$ ) atom (Ueda and Krouse, 1986). One method which uses a similar approach is known as “sulfur hexafluoride mass spectrometry” where the sulfur in a given sample is subjected to fluorine gas to get the sulfur into a gaseous phase as  $\text{SF}_6$  (Rumble et al. 1993). This method is usually more accurate than using  $\text{SO}_2$  due to the fact that fluorine has only one stable isotope ( $^{19}\text{F}$ ), so any variation in the mass of an  $\text{SF}_6$  isotopologue will be due to which sulfur isotope has been incorporated into the molecule (Rumble et al. 1993). The third method widely used by the source publications was Secondary Ion Microprobe Spectrometry (SIMS, also known as an “ion microprobe”; Mojzsis 2003). Here, a beam of ions (usually  $\text{Cs}^+$ ) is used to ionize the sulfur in a sample to be put through a mass spectrometer (Mojzsis 2003).

## Chapter 3. Reporting multiple sulfur isotope heterogeneities in the geologic record

I now review the theoretical considerations in reporting multiple sulfur isotope data. This section provides – in brief – the basis of isotopic geochemistry arguments (see Thiemens and Line 2019) for tracing the emergence of microbial sulfur metabolisms using data reported from the geologic record, and relate these changes to broader-scale transformations to the geosphere.

### 3.1 Conventional notations for the multiple sulfur isotopes

The four stable isotopes of sulfur ( $^{32}\text{S}$ ,  $^{33}\text{S}$ ,  $^{34}\text{S}$ ,  $^{36}\text{S}$ ) have the approximate terrestrial abundances of 95.03%, 0.7487%, 4.197%, and 0.01459%, respectively (Ding et al. 2001). These specific isotopic abundances were determined prior to the formation of our solar system via nucleosynthesis reactions in stars before they became incorporated into the building blocks of the planets (Mojzsis 2007). In reporting the chemistry of mass-dependent fractionation of multiple isotopes such as sulfur (Domagal-Goldman et al. 2011), we let  $a$  and  $b$  label the specific S isotopes,  $^a\text{S}$  and  $^b\text{S}$ , with  $a$  or  $b = [32, 33, 34, 36]$  as shown above, and  $a \neq b$ . In the hypothetical isotopic substitution reaction:  $^a\text{SA} + ^b\text{SB} \leftrightarrow ^b\text{SA} + ^a\text{SB}$  the equilibrium constant is expressed as:

$$K_{eq}^{ab} = \exp \exp \left( - \frac{\Delta E_{ab}}{kT} \right) = \frac{[^b\text{SA}]_{eq} [^a\text{SB}]_{eq}}{[^a\text{SA}]_{eq} [^b\text{SB}]_{eq}} . \quad [2]$$

Here,  $\Delta E_{ab} = E(^b\text{SA}) + E(^a\text{SB}) - E(^a\text{SA}) - E(^b\text{SB})$  is the free energy difference between reactant and product. From zero-point-energy arguments, it can be shown that  $\Delta E_{ab} \propto (1/\sqrt{m_a} + 1/\sqrt{m_b})$ . Since  $^{32}\text{S}$  is the lightest and most abundant isotope, we take it



as the reference, so that  $a = 32$ . When comparing three isotopes (e.g.  $^{32}\text{S}$ ,  $^{33}\text{S}$ ,  $^{34}\text{S}$ ) and because the mass differences of the isotopes are small, an approximation can be made:

$$\Delta E_{ab}/\Delta E_{ac} \approx (1/m_a - 1/m_b)/(1/m_a - 1/m_c) = \lambda_{eq} . \quad [3]$$

To report differences in the ratios of two isotopes (usually the most abundant, here  $^{32}\text{S}$  and  $^{34}\text{S}$ ), the conventional delta ( $\delta$ ) notation is used for mass-dependent isotopic fractionations. The mass-dependent sulfur isotopic compositions are expressed as part-per-thousand (0.1%; 1/1000; per mille; ‰) variations relative to a reference standard, as follows:

$$\delta^b S = \left[ \frac{(^bSA / ^{32}SA)_{\text{sample}}}{(^bSA / ^{32}SA)_{\text{standard}}} - 1 \right] \times 1000 \quad [4]$$

Where [Equation 4]  $b$  may refer to 33, 34, or 36, and  $\delta^b S$  is reported in units of ‰. The standard reference, which by definition is 0.00‰, is Vienna Cañon Diablo Troilite (VCDT). The VCDT standard is presently defined relative to a Ag-sulfide reference IAEA-S-1 with an agreed  $\delta^{34}\text{S}_{\text{VCDT}}$  value of -0.3‰.

Mass-dependent fractionation (MDF) represents the majority of processes within the sulfur isotope system. In MDF the isotopic ratios – ( $^{34}\text{S}/^{32}\text{S}$ ), ( $^{33}\text{S}/^{32}\text{S}$ ), ( $^{36}\text{S}/^{32}\text{S}$ ) – show systematic variability in proportion to the mass differences between the isotopes (Urey 1947; Hulston and Thode 1965). Hence, variations in ( $^{33}\text{S}/^{32}\text{S}$ ) of a sulfur-containing sample will be slightly more than half that of ( $^{34}\text{S}/^{32}\text{S}$ ) for the same sample. This is because the mass difference between  $^{33}\text{S}$  and  $^{34}\text{S}$  is the nucleon mass/energy difference between a neutron and a proton ( $M_p = 0.99862349M_n$ ). The resulting linear fractionation trends, commonly termed the terrestrial mass fractionation lines (TMFL), emerge from this mass difference with a slope of slightly more than 0.5.

$$\delta^{33}S = 0.515 \times \delta^{34}S \quad [5.1]$$

$$\delta^{36}S = 1.91 \times \delta^{34}S \quad [5.2]$$

Before the work of Farquhar et al. (2001), almost all sulfur isotope studies measured only ( $^{34}S/^{32}S$ ) because it was not expected that deviations in ( $^{34}S/^{32}S$ ) vs/ ( $^{33}S/^{32}S$ ) would occur in the rock record (cf. Thode et al. 1949; Riciputi et al. 1998). It is now widely understood that isotopic compositions that deviate significantly from the TMFL are preserved even in the oldest BIFs (e.g., Mojzsis et al. 2003). The deviations reflect mass-independent fractionation (MIF) processes of the S isotopes, and the Capital Delta ( $\Delta$ ) values are used to document this phenomenon. The definition for this phenomenon requires a second reference isotope, taken to be  $^{34}S$ . The general form is:

$$\Delta^b S = \delta^b S - [(1 + \delta^{34}S)^{b\lambda_{eq}} - 1], \quad [6]$$

Where  ${}^b\lambda_{eq} = (1/m_{32} - 1/m_b)/(1/m_{32} - 1/m_{34})$ . We know,  ${}^b\lambda_{eq} = \lambda_{eq}$  [Eqn. 3], and with the appropriate reference isotopes,  $a = 32$  and  $c = 34$ ; the mass differences lead to a slope value  ${}^{33}\lambda_{eq} = 0.515$ .

As with  $\delta$  values, MIF is expressed in the conventional notation on terms of  $\Delta^{33}S$  and  $\Delta^{36}S$  in parts-per-thousand (‰) deviations from the standard  ${}^{33}\lambda_{eq}$  slope, as:

$$\Delta^{33}S = \delta^{33}S - 1000 \times \left[ \left( 1 - \frac{\delta^{34}S}{1000} \right)^{0.515} - 1 \right] \quad [7.1]$$

$$\Delta^{36}S = \delta^{36}S - 1000 \times \left[ \left( 1 - \frac{\delta^{34}S}{1000} \right)^{1.91} - 1 \right] \quad [7.2]$$

Somewhat like the  $\delta$ -notation, *positive*  $\Delta^b S$  values ( $+\Delta^{33}\text{S}$  and  $+\Delta^{36}\text{S}$ ) indicate that a compound is anomalously enriched in that minor isotope, whereas a negative value points to depletion. The processes of MIF were so important on Earth prior to the Great Oxygenation Event (GOE) that it is misleading to term them as anomalous; these are reviewed below. Furthermore, although it seems that the sulfur MDF connotes  $\Delta^b S_{eq} = 0$ , we know that small differences in  ${}^b\lambda_{eq}$  can exist with different MDF processes or different standards (including VCDT) and different types of fractionations both abiotic and biotic (e.g., Farquhar et al. 2003). The inorganic reference materials show a narrow range in  $\Delta^{33}\text{S}$  of  $\pm 0.1\text{‰}$  ( $2\sigma$ ) about  $0\text{‰}$ . For example, Papineau et al. (2005) explained that this natural scatter in the standards statistically exceeds the internal analytical precision of the measurements. They proposed that these reflect additional sources of error, or the scatter may reflect real heterogeneity resulting from different modes of mass-dependent fractionation among the standards (Young et al. 2002). Values that fall more than  $3\sigma$  beyond a band in the TMFL about  $\pm 0.1\text{‰}$  from  $\Delta^{33}\text{S} = 0\text{‰}$  are interpreted as a signal of MIF.

### *3.2 MDF and MIF fractionation processes documented in the Archean sulfur cycle*

Different modes of isotopic fractionation produce sulfur compounds with diverse isotopic compositions, the combination of measured multiple isotopes ( $\delta$ ,  $\Delta$ ) described in **Chapter 3.1** can be used to identify the activity of these processes in deep time. Here, we turn our attention to some fractionation processes understood to have existed in the Archean surface sulfur cycle, the different isotopic signatures produced by those processes and how they can be understood in relation to the evolution of microbial metabolisms that utilize sulfur (either in reduced, or oxidized form). While other

fractionation processes are thought to have been active in Archean time, our discussion concerns those that are most relevant to understanding the early evolution of elemental sulfur utilization by life.

### *3.2.1 Atmospheric photochemistry and multiple sulfur isotopes*

Laboratory control experiments have shown that MIF sulfur isotopic signatures are produced by photolysis reactions with SO and SO<sub>2</sub> gas under ultraviolet lamps with wavelengths in the broadband 185-220 nm wavelengths under strictly anoxic atmospheres (Farquhar et al. 2000, 2001; Farquhar and Wing 2003). Modeling studies have sought to understand better the underlying mechanisms of this photochemistry in the Archean (Lyons 2009; Claire et al. 2014). These processes include photo-dissociation and/or photoexcitation (Lyons 2009). Authigenic sedimentary sulfur minerals (sulfides and sulfates) typically show characteristic non-zero  $\Delta^{33}\text{S}$  and  $\Delta^{36}\text{S}$  values, where  $\Delta^{36}\text{S}/\Delta^{33}\text{S} \approx -0.90$ , and  $\Delta^{33}\text{S}/\delta^{34}\text{S} \approx +0.73 \pm 0.15$  (Farquhar et al. 2001; Farquhar and Wing 2003; Thomassot et al. 2015); these slopes are referred to as the Archean Reference Arrays (ARA; **Figure 3**). It should be noted, however, that although the ARAs are commonly viewed as reliable MIF sulfur signals, other studies continue to investigate non-atmospheric causes for this phenomenon including reaction in aqueous solution or organic + aqueous mixtures (e.g., Lasaga et al. 2008; Watanabe et al. 2009; Whitehall and Ono 2012; Kumar and Francisco 2016).

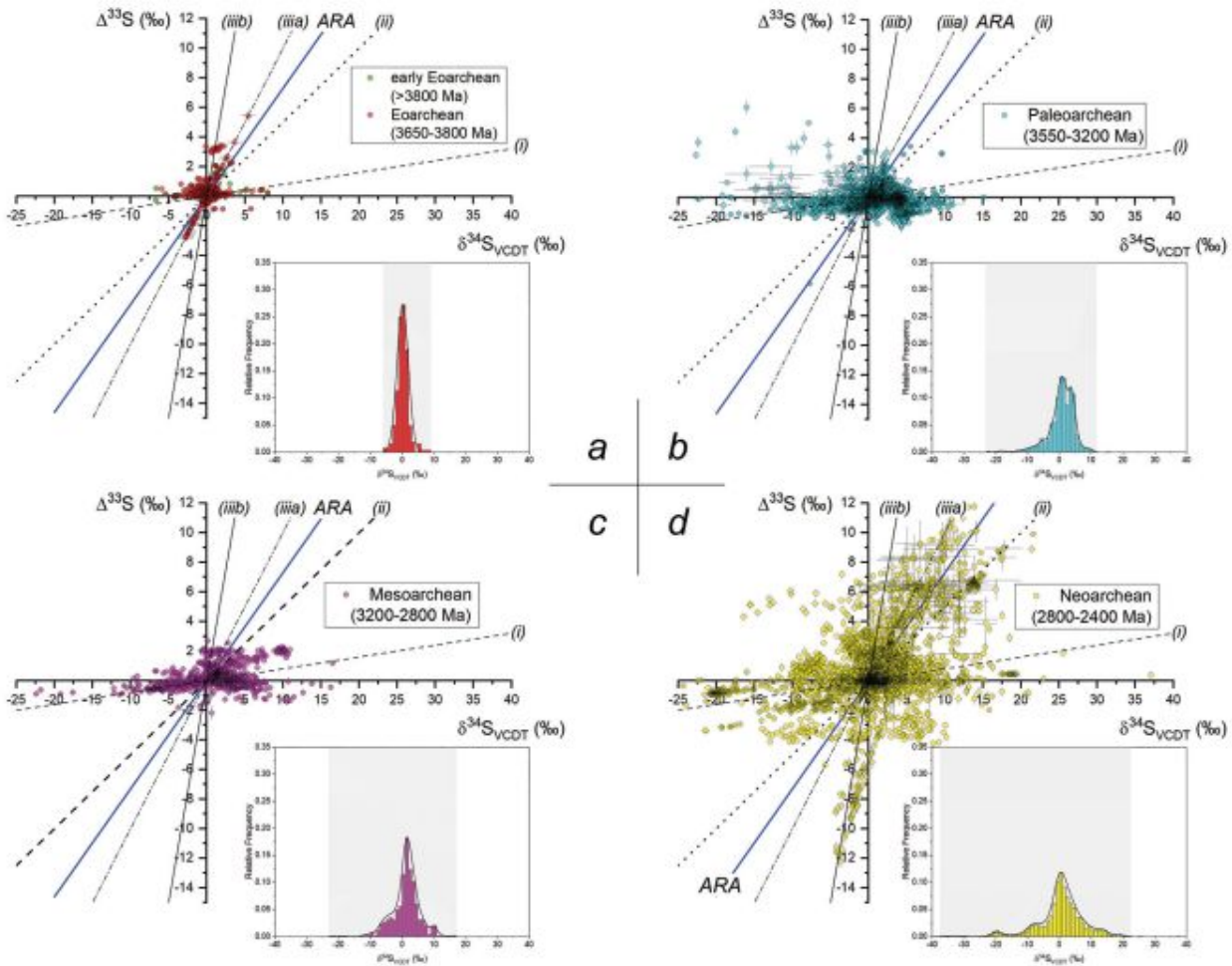


Figure 3. The multiple sulfur isotope record of different stages of the Archean. Here, we assess the relative influence of the different mass-independent fractionation trends via the  $\delta^{34}\text{S}$  vs.  $\Delta^{33}\text{S}$  relationship. The data are binned by age (a–d); generally, most mass-dependent Eoarchean data plot with  $\delta^{34}\text{S}$  near zero (inset, a), whereas ever increasing spreads in range of mass-dependent fractionation values as shown in the inset histograms characterize the Paleoarchean/Mesoarchean (similar) and Neoproterozoic records. a:  $\delta^{34}\text{S}$  vs.  $\Delta^{33}\text{S}$  data for Eoarchean [3650–3830 Ma], b: Paleoarchean [3200–3650 Ma], c: Mesoarchean [2800–3200 Ma], d: Neoproterozoic/early Paleoproterozoic [2400–2800 Ma]). Sulfur mass-dependent fractionation is expressed as  $\delta^{34}\text{S}$  V DCT on the x-axis, whereas mass-independent fractionation is reported in  $\Delta^{33}\text{S}$  on the y-axis. Also shown are the various documented mechanisms of atmospheric MIF sulfur production (see ‘Atmospheric photochemistry and multiple sulfur isotopes’ section). Labeled here are: ARA 1/4 Archean reference array; (i) photo-dissociation with self-shielding in a  $\text{SO}_2\text{-N}_2$  gas; (ii) photo-excitation; (iii) photo-excitation of self-shielded  $\text{SO}_2$  molecules in the 240–350 nm range from Whitehill and Ono (2012) and (iii b) from Ono et al. (2013).

Other mechanisms of atmospheric MIF sulfur production – besides the broadband ~200 nm UV array – have been explored to explain the records found in

ancient rocks (Lyons 2009). Beyond the ARA mentioned above, further experimental and numerical mechanisms for the various  $\Delta^{33}\text{S}/\delta^{34}\text{S}$  slope trends labeled in **Figure 3** that can be identified over the course of the Archean eon can be summarized as follows (Claire et al., 2014; Thomassot et al. 2015):

- (i) photo-dissociation with self-shielding in a  $\text{SO}_2\text{-N}_2$  gas [ $\Delta^{33}\text{S}/\delta^{34}\text{S} = +0.086 \pm 0.035$  (Ono et al. 2013)]
- (ii) photo-excitation [ $\Delta^{33}\text{S}/\delta^{34}\text{S} \approx +0.5$  (Hattori et al. 2013)]
- (iii) photo-excitation of self-shielded  $\text{SO}_2$  molecules in the 240- to 350 nm range [ $\Delta^{33}\text{S}/\delta^{34}\text{S}$  from  $\sim +1$  (Whitehill and Ono 2005) to  $+3$  (Ono et al. 2013)].

Corroborating evidence for a gas phase origin of these anomalous signatures also come from the observation of similar values in modern atmospheric sulfate aerosols and in sulfate from volcanogenic  $\text{SO}_n$  from Antarctic ice; in some cases these are correlated to historical volcanic eruptions that deliver sulfur gases to the stratosphere (Romero and Thiemens 2003; Savarino et al. 2003; Baroni et al. 2007). Owing to this body of evidence, photochemical transformations of  $\text{SO}_n$  are widely accepted as the cause of Archean MIF sulfur signatures even if other media are possible (cf. Kumar and Francisco 2016). The analyzed products – reduced and oxidized sulfur aerosols – of this UV induced photochemistry giving MIF S provide isotopic mass balance. The oxidized aerosol in this case, sulfate ( $\text{SO}_4^{2-}$ ), partitions sulfur isotopes such that it carries *negative*  $\Delta^{33}\text{S}$  and *positive*  $\Delta^{36}\text{S}$  values. Contrariwise, elemental sulfur aerosols ( $\text{S}^0$ ,  $\text{S}_{n+1}$ , cyclic  $\text{S}_8$ , polymeric S; Steudel 2003) carry *positive*  $\Delta^{33}\text{S}$  and *negative*  $\Delta^{36}\text{S}$ . We refer the reader to Claire et al. 2014 and Thomassot et al. 2015 for more about these phenomena.

### 3.2.2 Archean MIF sulfur aerosols, atmosphere transparency, low $pO_2$ , and scattering

As mentioned previously, controlled experiments show that low intrinsic oxygen concentrations and specific UV wavelengths that penetrate deep into the atmosphere are required to produce and preserve widespread MIF sulfur signatures in the geologic record. Ozone and oxygen are the primary absorbers of UV at wavelengths less than 300 nm, including those wavelengths involved in the photochemical reactions described in the previous section.

To account for the observed pervasive MIF sulfur in the pre-GOE geological record and its continuum from the end of the Hadean to the Paleoproterozoic (with the possible exception of the Mesoarchean; Thomassot et al. 2015), Mojzsis (2007) argued that Earth's atmosphere must have had the following properties: (i) transparent to short wavelength UV radiation and not so dense (e.g.  $\ll 0.5$  bar  $CO_2$ ) that Einstein-Smoluchowski scattering attenuates UV photons and prevent them from penetrating deep into the atmosphere and (ii) low in atmospheric  $pO_2$  to mitigate formation of an ozone screen, as well as to prevent production of significant marine sulfate to dilute a MIF sulfur signal. Pavlov and Kasting (2002) calculated that the effective transfer of MIF via reduced sulfur species ( $S^0$  to polymeric  $S_{n+1}$ ) from the atmosphere to the oceans requires that the early atmosphere had  $pO_2$  values  $\ll 10^{-5}$  present atmospheric levels (Lyons et al. 2014).

The undoubtedly abundant MIF  $S_{n+1}$  aerosols in the Archean serve as excellent tracers of the early evolution of the biogeochemical sulfur cycle, and I use this fact to explain  $\Delta^{33}S/\delta^{34}S$  data in the context of the emergence of different styles of metabolic

cycling of sulfur. I now direct our attention in this work to elemental sulfur aerosols that carry *positive*  $\Delta^{33}\text{S}$  and for which the most MIF S data are available; I therefore limit further discussion to the  $\Delta^{33}\text{S}/\delta^{34}\text{S}$  system. At the present time, the  $\Delta^{36}\text{S}$  systematics are still limited as long as relatively fewer data are available for  $^{36}\text{S}/^{32}\text{S}$  for ancient rocks.

### 3.2.3 Using polar coordinates to interpret multiple S-isotope data

Conventionally, sulfur isotope data over the course of the Archean has used  $\Delta^{33}\text{S}$  as a proxy for the quantity of UV photolysis that has occurred over time (**Figure 3 A**) (Mojzsis, 2007). While straightforward, this method has potential shortcomings due to the fact that the 193nm photolysis array induces a stronger fractionation of  $\Delta^{33}\text{S}$  while the broadband 190-220 nm array has a stronger impact on  $\Delta^{36}\text{S}$  (Farquhar et al. 2001; Ono et al 2013). As such, using  $\Delta^{33}\text{S}$  as a proxy will make samples subjected to 193 nm wavelengths appear to have undergone more photolysis than they have relative to the broadband wavelength. Therefore, one possible method to correct for this is to use the “hypotenuse” of the  $\Delta^{33}\text{S}$  and  $\Delta^{36}\text{S}$  values to indicate the relative quantity of photolytic fractionation to which the sample was subjected to. This information can be combined with the angle of the slope of each data point from the origin ( $\Delta^{33}\text{S}$  and  $\Delta^{36}\text{S} = 0$ ) (Farquhar et al. 2001) to indicate which wavelengths were inducing photolysis. Although the convention has been to use the slope, when representing the totality of the data, individual points near the origin can have very high absolute values, collapsing the resolution between 1 and -1. Instead, a polar coordinate system can be used where the distance from the origin represents to what quantity of photolysis the sample has been subjected to and the angle of the slope is used to determine which wavelengths it was subjected to. Using the angle will result



in all data points falling between 90° and -90°, minimizing distortion and allowing the nature and intensity of UV photolysis to be illustrated across large periods of time. The following equations describe the quantity to which a sample has been subjected to MIF where X describes an element (such as S) and i and j represent the atomic mass of specific isotopes (33 and 36 in this case).

$$\Delta^rX = (\Delta^iX^2 + \Delta^jX^2)^{-5} \quad [8.1]$$

$$\Delta^rS = (\Delta^{33}S^2 + \Delta^{36}S^2)^{-5} \quad [8.2]$$

The following equations describe how the angle of the array the sample is on.

$$\Delta^\theta X = \tan^{-1}(\Delta^jX/\Delta^iX) \quad [9.1]$$

$$\Delta^\theta S = \tan^{-1}(\Delta^{36}S/\Delta^{33}S) \quad [9.2]$$

When looking at the  $\Delta^{33}S$  values of the early Archean period, the MIF intensity of the Paleoarchean seems somewhat higher than the Eoarchean (**Figure 3a**). This could lead one to conclude that the sudden utilization of elemental sulfur in the Paleoarchean may result from an increase in the production of photolytically produced elemental sulfur. However when multiple isotope data are used, a somewhat different pattern emerges. The  $\Delta^rS$  of the Eoarchean sulfides is similar to those of the Paleoarchean with the Paleoarchean values clustering around the 193 nm angle while those in the Eoarchean are between the 193 nm and 190-220 nm angle. This again suggests that high array angles reduced the MIF signal of the Eoarchean. It also suggests most of the UV spectrum was acting on volcanic sulfur dioxide in the Eoarchean yet virtually all wavelengths except the 193 nm were filtered in the

Paleoarchean (Mueller et al. 2016). Such a similar trend has been observed when looking at  $\Delta^{33}\text{S}$  along with  $\delta^{34}\text{S}$  values and one explanation put forth is that carbonyl sulfide in the atmosphere shielded the broadband wavelengths (Mueller et al. 2016). This then raises the question, why did the OCS levels increase in the atmosphere at this time? One explanation may be related to the rise of methanogens near the end of the Eoarchean (Ueno et al. 2006). Methane can undergo photooxidation to form carbon monoxide (Schwieterman 2019) that will then react with sulfur dioxide to form OCS (Mueller et al. 2016).

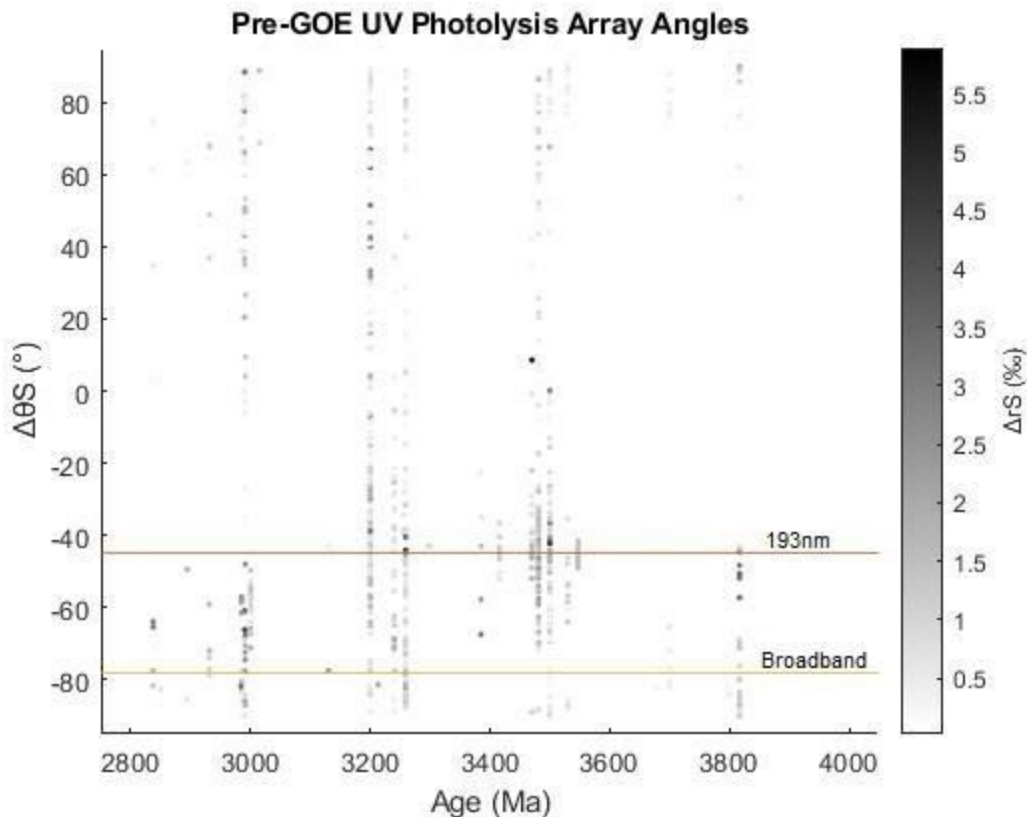


Figure 4: Polar coordinate plot of Eo-Mesoarchean MIF sulfur isotope record (Neoproterozoic omitted to increase resolution of the data points of the time in question). The two horizontal lines indicate the positions of the 193nm and 202nm or “broadband” photolysis arrays.

### 3.3 Archean sulfur metabolisms

Of the various microbial sulfur metabolisms proposed to have been active in the Archean eon (e.g., Shen et al. 2001, 2009; Wacey et al. 2010; Guy et al. 2012; Eickmann et al. 2018), I direct our analysis to the *sulfur reducers*, *oxidizers* and *disproportionators* (*elemental sulfur fermenters*). I refer the reader to recent reviews (e.g., Maier 2015) for more details about the nature of the sulfur biogeochemical cycles, to Rabus et al. (2013) for sulfur metabolisms and to Dahl (2017) for a comprehensive analysis of phototrophic sulfur metabolism.

#### 3.3.1 Mineralogical aspects of microbial “sulfate reduction”

“Sulfate-reducing” microbes actually metabolize  $\text{SO}_4^{2-}$  transformed to  $\text{SO}_3^{2-}$  by ATP activation, or formation of sulfite (and bisulfite;  $\text{HSO}_3^-$ ) by reaction of  $\text{SO}_2$  in water, to produce product sulfide- and polysulfide ( $\text{S}_n^{2-}$ ) that in turn reacts in water to form metal sulfide (**Figure 3: Chapter 2.3.1**) This subsequently goes on to become incorporated into sediments. The general exergonic part of sulfate reduction is sulfite reduction (or sulfur reduction) to  $\text{H}_2\text{S}$ . In the geobiological literature, this reaction is commonly expressed as:



where  $\text{CH}_2\text{O}$  is taken as generic “organic matter” (Berner 1985) and the implication is that  $\text{SO}_2$  forms  $\text{SO}_3^{2-}$ , which can also be used in lieu of  $\text{SO}_4^{2-}$ . Microbes that perform microbial sulfate reduction (MSR) preferentially metabolize  $^{32}\text{S}$ -compounds relative to  $^{34}\text{S}$ -compounds, which leads to mass-dependent depletions in  $^{34}\text{S}$  vs.  $^{32}\text{S}$  and consequently negative fractionations in the  $\delta^{34}\text{S}$  of the product sulfide (Thode et al. 1951; Jones and Starkey 1957; Harrison and Thode 1958). Analysis of modern

sedimentary environments show that these isotopic fractionations can be up to ~50‰ (Goldhaber and Kaplan 1975; Canfield 2001).

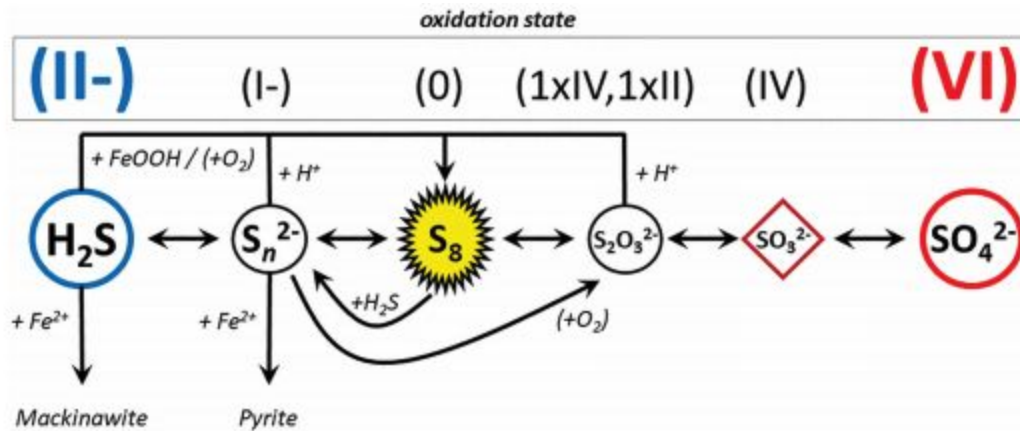
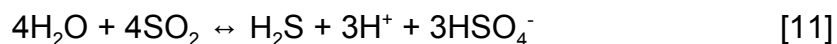


Figure 5. Schematic diagram of inorganic sulfur redox reactions in the marine system related to source and valence state (see Figure 1). The central role of elemental sulfur/polysulfide (aerosol) in controlling intermediate sulfur species transitions as well as Fe-sulfide mineralization is emphasized in this conceptual framework (modified from Kafantaris and Druschel 2020).

Sulfide minerals can be produced by the reaction of MSR-produced H<sub>2</sub>S [Eqn. 8] with Fe(II)<sub>aq</sub> to form precursor amorphous [FeS]<sub>aq</sub> and thence to intermediates such as mackinawite ((Fe,Ni)<sub>1+x</sub>S (where x = 0 to 0.11)) which transforms at low temperature diagenesis to greigite ((Fe<sup>2+</sup>Fe<sup>3+</sup>)<sub>2</sub>S<sub>4</sub>), and the orthorhombic polymorph marcasite (FeS<sub>2</sub>) to the cubic mineral (FeS<sub>2</sub>) pyrite (e.g., Schoonen and Barnes 1991; Avetisyan et al. 2019). Sulfur metabolically processed in MSR means that these minerals preserve a memory of the biological involvement by carrying strongly *negative* δ<sup>34</sup>S (Berner 1970, 1984). I return to this later (**Chapter 3.3.2**), but it is well established that sediments deposited in Archean environments preserve δ<sup>34</sup>S fractionations that are typically <20‰ (Sim et al. 2019), and for Eoarchean rocks of sedimentary protolith like BIFs, they are

much less than that ( $\leq 10\%$ ). This overall trend in mass-dependent sulfur isotopes is interpreted to mean that  $\text{SO}_4^{2-}$  concentrations in the Archean oceans were very low, and that MSR was unable to operate in the general absence of reactive sulfate (e.g., Fike et al. 2014).

The exception to sulfate-absent Archean oceans is the localized stabilization of  $\text{SO}_4^{2-}$  by fluids interacting with, for example, silicic magma chambers with associated caldera collapse and seawater incursions. These partially isolated environments will locally evolve highly oxidized (Scaillet et al. 1998) and volatile-rich saline fluids (Newton and Manning 2005) and the expulsion of these oxidized fluids stabilize  $\text{SO}_2$ . Confined to a regional volcano-sedimentary environment the  $\text{SO}_2$  hydrolysis reaction (Hattori and Cameron 1986):



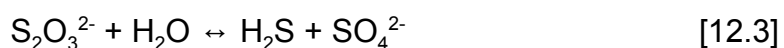
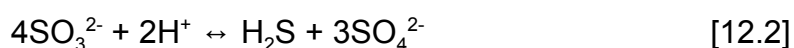
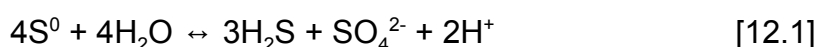
yields sulfate even without free oxygen in the system, which then converts to (bi)sulfite (viz. Eqn 8). Other products in this reaction are hydrogen sulfide and free hydrogen. For instance, microscopic sulfide (pyrite) grains co-exist with sulfates in the ca. 3.49 Ga barite (barium sulfate;  $\text{BaSO}_4$ ) beds from the Dresser Formation, Warrawoona Group at North Pole in Western Australia (Philippot et al. 2007). These rocks formed at a time when there should have been no sulfate in ambient seawater. Underscoring how unusual these rocks are, sedimentary sulfates do not appear again in the rock record until about a billion years later in the Neoproterozoic (e.g., Zhelezinskaia et al. 2014).

Fractionations by MSR of the minor isotope  $^{33}\text{S}$  have been recorded to yield relatively higher  $^{33}\text{S}/^{32}\text{S}$  in product sulfide (e.g., Johnston et al. 2005; Ono et al. 2006).

This process also, interestingly, results in small positive  $\Delta^{33}\text{S}$  values. It is worth noting that this same process discriminates against  $^{36}\text{S}$ , and thus to negative  $\Delta^{36}\text{S}$  in the sulfide product relative to the starting values of the sulfate reactant. Johnston et al. (2007 and references therein) also reported  $\Delta^{36}\text{S}/\Delta^{33}\text{S}$  of  $\sim -6.9$ , with the magnitude of the changes in  $\Delta^{33}\text{S}$  and  $\Delta^{36}\text{S}$  observed to scale with degree of mass dependent fractionation in  $\delta^{34}\text{S}$ .

### 3.3.2 Mineralogical aspects of microbial sulfur disproportionation

Microbial sulfur disproportionation (MSD) is a form of fermentative metabolism that uses sulfur in a series of redox reactions to generate  $\Delta G^\circ$ . Organisms metabolize sulfur intermediate compounds such as elemental sulfur ( $\text{S}^0$  and sulfur polymers) and sulfite ( $\text{SO}_3^{2-}$ ) to produce sulfide and sulfate as products (Bak and Pfennig 1987; Canfield and Thamdrup 1994; Thamdrup et al. 1994; Canfield and Teske 1996; Finster et al. 1998; Cypionka et al. 1998; Habicht et al. 1998; Rabus et al. 2013). The disproportionation of inorganic sulfur intermediates can be done with or without free hydrogen present in the system. The general forms of these reactions are:



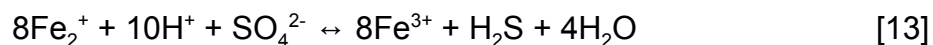
Culture studies have shown that elemental sulfur disproportionation [Eqn. 12.1] typically concentrates  $^{32}\text{S}$  in the sulfide product that in turn leads to mass-dependently fractionated negative  $\delta^{34}\text{S}$  values between 5.5 – 11.3 ‰ (Canfield et al. 1998). In another culture study by Johnston et al. (2005) it was shown that the opposite sign can also occur, with positive fractionations in  $\delta^{34}\text{S}$  up to  $\sim 4$  ‰. Analyses of sulfite

disproportionation reactions (displayed in the aforementioned equations) also show that the product sulfide is depleted in  $^{34}\text{S}$  and the sulfate product is enriched in  $^{34}\text{S}$  (Habicht et al. 1998). Authenticated fractionations in sulfide  $\delta^{34}\text{S}$  are between +20 and +45 ‰, and the sulfate shows  $\delta^{34}\text{S}$  negative fractionation of -7 to -12 ‰ (Johnston et al. 2005). Very few data are currently available to allow us to confidently evaluate how  $\Delta^{33}\text{S}$  values change in the sulfite disproportionation process; what does exist indicates that values of both products show *increases* in  $^{33}\text{S}$  relative to the reactant  $\text{SO}_3^{2-}$ .

### 3.3.3 Post-depositional abiotic sulfur isotope fractionation processes

Thermochemical sulfate reduction (TSR) is thought to have been an active process within the Archean sulfur cycle even as it requires the presence of reactive sulfate (e.g. Jamieson et al. 2013). The TSR process may refer to either abiotic reduction of sulfate where  $\text{Fe}^{2+}$  acts as an electron donor (hereafter,  $\text{TSR}^1$ ), or reduction of sulfate by organic carbon ( $\text{TSR}^2$ ). These reactions happen at higher temperatures than MSR (**Chapter 3.2.1**), which has an optimal temperature range between  $\sim 20^\circ\text{-}40^\circ\text{C}$  (Jørgensen et al. 1990; Sageman et al. 1998; Canfield 2001). The two forms of TSR described above have been invoked to explain some features of the Archean sulfur cycle.

The  $\text{TSR}^1$  process uses  $\text{Fe}^{2+}$  and free hydrogen  $\text{H}^+$  (**Chapter 3.3**) and occurs at temperatures of  $\sim 200^\circ\text{-}350^\circ\text{C}$  (Trudinger et al. 1985), via:



Isotope fractionation models (Janecky and Shanks 1988) show that the reaction leads to product sulfide concentrated in  $^{34}\text{S}$  with positive fractionations of  $\delta^{34}\text{S} \geq 5\text{‰}$ . It

is still unknown how this process [Equation 13] affects fractionation in the minor isotopes, if at all. In the geologic record, TSR<sup>1</sup> is usually recognized where sulfides that host negative  $\Delta^{33}\text{S}$  values requiring the reduction of MIF sulfate to sulfide preserving the mass-independent signal, occurs within high temperature chemical environments in the crust such as the volcanogenic massive sulfide (VMS) deposits (e.g., Jamieson et al. 2006, 2013; Bekker et al. 2009).

The TSR<sup>2</sup> involving organic matter – which itself is abundant in hydrogen – commonly takes place at temperatures of ~100°-140°C and up to about 180°C (Machel 1998; Claypool and Mancini 1989) in a mechanism resembling that in [Eqns. 9, 12.2]. Experiments have verified that the TSR<sup>2</sup> mechanism concentrates <sup>32</sup>S in the product sulfide and produces negative  $\delta^{34}\text{S}$  fractionations between ~0 and 10‰ (Kiyosu 1980). Intriguingly, Watanabe et al. (2009) also showed that the product  $\Delta^{33}\text{S}$  values are ~0.1 – 2.1‰ higher than that of the reactant sulfate.

Now that I have reviewed the general manner of microbial and abiotic sulfur isotopic fractionations, they can be placed in the context of the early evolution of the sulfur cycle and its bearing on the record of microbial metabolic evolution in the Archean marine reservoirs.

### *3.4 Microbial sulfur reduction in the Archean marine system*

Sulfur reservoirs in the marine system can be divided into three main components: Marine sediments, seafloor hydrothermal environments and seawater (aqueous) sulfate. Sulfide minerals can be found in rocks from each of these components in the geological record. Such sulfides carry *positive*  $\Delta^{33}\text{S}$  values and



relatively large *positive* or *negative*  $\delta^{34}\text{S}$ ; where these values deviate from the ARA in  $\Delta^{33}\text{S}/\delta^{34}\text{S}$  space (**Chapter 3.2.1**), they are typically ascribed to the action of MSD in the Archean (e.g., Wacey et al. 2010). This relationship in  $\Delta^{33}\text{S}/\delta^{34}\text{S}$  space is illustrated in **Figure 3b** for the Paleoarchean sulfides with a noticeably wider range in  $\delta^{34}\text{S}$  (inset) than in the preceding Eoarchean.

### 3.4.1 Authigenic sulfide mineral formation in Archean banded iron-formations

Banded iron-formations are characteristically laminated Fe-rich (~20 to 40 wt.% Fe) siliceous (~40 to 50 wt.%  $\text{SiO}_2$ ) sedimentary rocks that formed extensively in the oceans throughout the first 2 billion years of Earth history (James 1954). The formation of BIF was perhaps modulated by life (Kappler et al. 2005), which would qualify the rock type as a biomarker. At time of sedimentation, the primary Fe-mineralogy of the BIFs included hydrated ferric oxy-hydroxides ( $\text{Fe}^{3+}\text{O}(\text{OH}) \cdot n\text{H}_2\text{O}$ ), the serpentine-group mineral greenalite ( $\text{Fe}^{2+}, \text{Fe}^{3+}$ )<sub>2-3</sub>  $\text{Si}_2\text{O}_5(\text{OH})_4$ , and the ferrous-carbonate mineral siderite ( $\text{Fe}^{2+}\text{CO}_3^{2-}$ ) (Han 1966). Subordinate primary minerals included sulfide, (basic calcium) phosphate, and organic matter (Klein 2005). It is also probable that the oceans at that time were enriched in dissolved silica (Konhauser et al. 2007) and under such conditions the precipitation of amorphous silica can take place directly on the sea floor out of solution. Consequently, this would add silica to the list of primary minerals in BIFs (Krapež et al. 2003). Depending on the degree of metamorphism, the most common sulfide minerals present in BIF are pyrite ( $\text{FeS}_2$ ; **Figures 1, 5**) and its high-temperature (metamorphic) polymorph pyrrhotite ( $\text{Fe}_{1-x}\text{S}$  [where,  $x = 0$  to 0.2]).

As previously discussed (**Chapter. 3.2.2**) characteristic *positive*  $\Delta^{33}\text{S}$  and *negative*  $\Delta^{36}\text{S}$  values of Archean sulfides are indicative of the reduced, MIF elemental

sulfur aerosols that were transported to the oceans, converted to sulfide and subsequently preserved in sediment (e.g. Izon et al. 2015).

My focus is mainly on the geological record of BIFs, because they are the most abundant (preserved) of all Eo- to Paleoproterozoic sediments (Klein 2005). Yet, how were the MIF elemental sulfur aerosols converted to sulfide and incorporated into sulfide minerals? The possible mechanism depends on whether it was biologically modulated or not.

A plausible path for this process is via H<sub>2</sub>S production from S<sup>0</sup> in MSD [Eqn. 8.1], followed by what has been proposed as a direct reaction of product sulfide with abundant [Fe<sup>2+</sup>]<sub>aq</sub> in the Archean oceans (Holland 1973, 1984), as in:



Note that Schoonen and Barnes (1991), Canfield and Thamdrup (1996), and Pyzik and Sommer (1981) provide important caveats about sulfide saturation in the simple scenario [Eqn. 11].

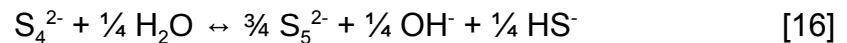
Alternatively, elemental sulfur aerosols (S<sup>0</sup>, S<sub>n+1</sub>, cyclic S<sub>8</sub>, polymeric S<sub>x</sub><sup>2-</sup>) can react *directly* with ferro-ferric oxy-hydroxides; these were abundant in solution in the Archean oceans (e.g., Arrhenius et al. 1993). The relevant reaction is:



Here, the reactivity of aqueous Fe<sub>3</sub>(OH)<sub>8</sub> with elemental sulfur produces hydrogen. The compound Fe<sub>3</sub>(OH)<sub>8</sub> is a mixed-valence iron oxy-hydroxide dubbed ferrosic hydroxide (Arden, 1950); it is an unstable precursor to magnetite in ferruginous sediments. Ferrosic hydroxide belongs to a mineralogical family of mixed valence compounds

termed *Green Rusts* that have general compositions varying from  $\text{Fe}_2(\text{OH})_5$  (Trolard et al. 1997) to  $(\text{Fe}^{2+}_{(1-x)}\text{Fe}^{3+}_x - (\text{OH})_2)^{x+} (x/n\text{A}^{n-} m/n\text{H}_2\text{O})^{x-}$  (Genin et al. 1998), where A can be substituted by the anions  $\text{OH}^-$ ,  $\text{Cl}^-$ ,  $\text{CO}_3^{2-}$ , or  $\text{SO}_4^{2-}$ . Several studies have implicated the *Green Rust* precursor minerals as the feed stocks of the magnetite found in the Archean BIFs (Kuma et al. 1989; Arrhenius 2003; Halevy et al. 2017).

A further pyrite-forming pathway to consider is the polysulfide reaction wherein pentasulfide ( $\text{S}_5^{2-}$ ) reacts with FeS to give  $\text{FeS}_2$  and  $\text{S}_8$  (Rickard and Luther, 2007; Kafantaris and Druschel 2020). Polysulfides ( $\text{S}_x^{2-}$ ;  $x = 2$  to 8 in natural systems; Kamyshny et al. 2004) in my case come into play via the abundant  $\text{S}^0$  aerosols known to exist and traced by MIF from atmospheric reactions on the early Earth (**Chapter 3.2.1**). Intriguingly, chain-length distribution of the  $\text{S}^0$  aerosols in aqueous systems is determined by disproportionation reactions, principally:



Whereupon the pentasulfide reacts to form pyrite.

### 3.4.2 Secular $\delta^{34}\text{S}$ trends in Eoarchean-Paleoarchean sulfides

Notably for my work, the geological record of  $\delta^{34}\text{S}$  fractionations for Eoarchean sediments in **Figure 3a** (see inset) shows that this mass-dependent process was subdued; Eoarchean sulfur isotopes preserve small  $\delta^{34}\text{S}$  fractionation values ascribable either to abiotic processes (**Chapter 3.2.3**) or perhaps to a simple form of elemental sulfur reduction (Kaplan and Rittenberg 1962). The earliest evidence for MSD as reported in Philippot et al. (2007) and Mojzsis (2007), takes the form of pyrite with *positive*  $\Delta^{33}\text{S}$  values and where these values begin to significantly deviate from the ARA

in  $\Delta^{33}\text{S}/\delta^{34}\text{S}$  space is in the Paleoproterozoic record and afterwards (**Figures 3b-c; insets**). By Neoproterozoic time (**Figure 3d, inset**) the sulfur isotopes are strongly mass-dependently fractionated.

Eoproterozoic sulfides are characterized by a very narrow range of  $\delta^{34}\text{S}$  values (inset, **Figure 3a**) that points to minimal fractionation between sulfate and sulfide (**Figure 5**) with the important caveat that no data are thus far available from the paired sulfate-sulfide samples necessary to constrain this fractionation (Fike and Grotzinger 2008; Fike et al. 2006, 2014; Gill et al. 2011). Geochemical studies and laboratory microbial culture work to explore the impact of sulfate concentration on fractionation during microbial sulfate reduction, show that such reduced  $\delta^{34}\text{S}$  fractionations in sedimentary sulfur minerals is evidence for sulfate abundances sufficiently low (<200  $\mu\text{M}$ ) to inhibit any fractionation during that time (Habicht et al. 2002). Other results (Crowe et al. 2014; Zhelezinskaia et al. 2014) suggest even lower ambient sulfate levels (<10  $\mu\text{M}$ ) in the early Archean (**Chapter 3.3.1**).

Furthermore, high-resolution spatial analysis by secondary ion mass spectrometry (SIMS; ion microprobe) of Archean pyrites documents higher fractionations than are apparent from bulk  $\delta^{34}\text{S}$  pyrites (Mojzsis et al. 2003; Kamber and Whitehouse 2007). These preserved micrometer-scale  $\delta^{34}\text{S}$  differences occur in pyrites that also preserve mass-independent signatures. These data confirm that the variable fractionations in  $\delta^{34}\text{S}/\Delta^{33}\text{S}$  within Eoproterozoic to Paleoproterozoic sedimentary pyrites are primary and not the result of later-stage overprinting (Watson et al. 2009).

## Chapter 4. Evolution of biological sulfur cycling on the Eoarchean to Paleoarchean Earth

Next, I explore how the genes involved in sulfur metabolism may have evolved on the Eoarchean to Paleoarchean/Mesoarchean Earth to account for the observed trends in the multiple sulfur isotope data.

### *4.1 Eoarchean alkaline hydrothermal vents as a waystation for early life*

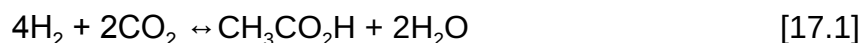
The microbial community that composed LUCA may have included a hydrogenotrophic acetogen with a primordial metabolism utilizing the Wood-Ljungdahl pathway (Russell and Martin 2004, Weiss et al. 2016). To better understand the nature of this early biosphere, modern analogue environments conventionally serve as a guide. Enzymes involved in the W-L pathway have many cofactors that resemble minerals involved in the abiotic synthesis of organic molecules in alkaline hydrothermal systems (Russell et al. 2013). Here I propose that these chemically dynamic environments as a *salle d'attente* for emergent life and a gateway for the colonization of the oceans.

I have reiterated the case that at least at some transitional stage Earth's Eoarchean-Paleoarchean biosphere included a biome that primarily resided in alkaline hydrothermal vent systems. The deepest-rooted forms of metabolism have a similar series of reactions that are identified to occur in mafic (alkaline) hydrothermal vents, whether on the seafloor or the shallow subsurface and comparative biochemistry has indicated that LUCA possessed a metabolism similar to those present in organisms that inhabit alkaline vents (Weiss et al. 2016). It is interesting to note that even on the contemporary Earth, a combination of biotic and abiotic carbon fixation reactions can

take place within these environments (e.g., Martin and Russell 2006). Further, the presumed biogenic carbonaceous materials measured in sediments from such environments have a  $\delta^{13}\text{C}$  range of -28.9‰ to -21.5‰, whereas postulated abiogenic carbon varies from -15‰ to -9‰ (Proskurowski et al. 2008); this range is similar to that observed in Eoarchean rocks ascribable to evidence of past biological activity (Papineau et al. 2010; Havig et al. 2017). As I argue later, by approximately Paleoarchean time, data from the rock record seem to indicate that life went from exclusive hydrogenotrophic carbonate reduction to a variety of metabolisms including methanogenesis (e.g., Ueno et al. 2006), photosynthesis (e.g., Olson 2006) and respiration (e.g., Bontognali et al. 2012). This evolution towards metabolic complexity is the natural consequence of life's dependence on non-equilibrium electron transfers (Falkowski, 2006).

If alkaline hydrothermal vents were a stepping stone for early life (see Martin 2016 for a summary), we may inquire what happened as more metabolic pathways emerged in this environment? Biosynthetic pathways that would have produced materials needed for metabolism (such as nucleic acids and enzyme cofactors) were at first synthesized via abiotic processes (e.g., in the serpentinization environment) and inherited by the earliest organisms (Wang et al. 2014). Such early emergent biosynthetic pathways ought to include those involved in ever more sophisticated amino and nucleic acid biosynthesis, which would lead to an ever greater chemical distinction between the portions of the hydrothermal crucible where biogenic and abiogenic carbon reduction took place (e.g., Martin and Russel 2006). Once hydrogenotrophic acetogenesis [Equation 17.1] was firmly established by this nascent biome (see, for

example, Fig. 1 of Martin 2016), it set the stage for diversification into methanogenesis [Equation 17.2]; this increased the total energy obtained from carbonate reduction. Furthermore, the origin of fermentative heterotrophs would have allowed organisms to derive energy from previously reduced carbon by converting said compounds into the most thermodynamically favorable configuration (Schönheit et al. 2016) [Equation 17.3].



The evolution of biosynthetic pathways would have allowed life to survive throughout an alkaline vent, I argue that it would still be limited to near-vent niches for reliable access to the mineral precursors of the functional groups used to catalyze metabolism. Only after gaining the ability to synthesize these cofactors from more and more simple starting materials, could organisms venture forth beyond the hydrothermal cradle into the surrounding marine habitats. That is, if the required raw materials, hydrogen and inorganic carbon, were present for a relocation (Holliday et al. 2007).

#### *4.2 Environmental availability of free hydrogen*

A number of natural mechanisms are available to provide crustal  $\text{H}_2$  to the environment (e.g., Morita 2000) [Equation 1], but an important caveat to these various sources is that the hydrogen must be at least at the minimum abundance levels required for  $\text{H}_2$ -dependent growth (Schink 1997; Thauer et al. 2008). This is a challenge because hydrogen gas in the environment is ephemeral with very fast diffusion times. Free hydrogen can be formed in relatively low oxygen fugacity (dissolved-gaseous

equilibrium) reactions between dissolved gases in the system C-H-O-S in magmas, especially in those with basaltic affinities that continuously form and sustain hydrothermal vents; by thermal decomposition of organic matter and  $\text{CH}_4$  to  $\text{C}^0$  and  $\text{H}_2$  at temperatures around  $600^\circ\text{C}$ ; via reaction between  $\text{CO}_2$ ,  $\text{H}_2\text{O}$ , and  $\text{CH}_4$  at elevated temperatures in the vapor phase; from radiolysis of water by U and Th, and their radioactive (intermediate) daughters, and potassium-40; catalysis of silicates under stress in the presence of water; hydrolysis of ferrous minerals in ultramafic rocks (peridotite, komatiite); and, mantle exhalations via volcanic or passive crustal out-gassing. These various sources of hydrogen are frequently misconstrued to mean that there is no strong limitation to free hydrogen availability for metabolism. Of the endogenous sources,  $\text{H}_2$  from vents and the serpentinization process is the most important. Methanogens and acetogens and  $\text{H}_2$ -dependent microbes in general need on the order of 1-10 Pa  $\text{H}_2$  for the metabolic reaction to be exergonic. It is for this reason they grow near serpentinizing systems, or occur together with  $\text{H}_2$ -producing fermenters. To underscore this point, it is not enough that free hydrogen can be made at the crust-hydrosphere interface, it must be at adequate abundance to be useful (e.g., Orsi et al. 2020).

Once a dependable capacity to produce the organic and inorganic molecules could be found to sustain cellular metabolism away from a reliable source of  $\text{H}_2$  and mineral precursors at alkaline hydrothermal vents, later microbial life was no longer confined to these environments. Yet, an interesting challenge for early life arises: sulfur oxides ( $\text{SO}_n$ ;  $n=1,2,3$ ) released by volcanic and passive outgassing in active



hydrothermal regions quickly react with water to form bisulfite ( $\text{HSO}_3^-$ ) and thence sulfite ( $\text{SO}_3^{2-}$ ) as in:



The product [Eqn. 18.2] can be oxidized further to form sulfate ( $\text{SO}_4^{2-}$ ), or sulfuric acid ( $\text{H}_2\text{SO}_4$ ) depending on the pH (e.g. Ranjan et al. 2018). In the absence of available oxygen to deep Eoarchean-Paleoarchean hydrothermal environments, the bulk of the sulfur (Rimmer and Shorttle 2019) will be in the form of bisulfite ( $\text{HSO}_3^-$ ) and hydrogen sulfide ( $\text{HS}^-$ ). Sulfite is highly reactive and requires detoxification by microbes (**Chapter 4.4.1**)

#### *4.3 Selective pressures on the early biochemical evolution of sulfur metabolism*

The ability to metabolize elemental sulfur would not have emerged *de novo*; it must have evolved from an existing enzyme that was already integrated into a metabolic system (Duval et al. 2008). To understand why it was delayed until the Paleoarchean, we must understand what metabolic systems and what environmental conditions were present to account for this delay. While data indicate that ESR was operative by 3.5 Ga (Philippot et al. 2007), molecular evidence are at odds with this being the oldest form of sulfur metabolism; other forms of sulfur metabolism were there first (Duval et al. 2008). Phylogenetic evidence shows that some of the genes involved in respiratory sulfur metabolism were present in the LUCA microbial community (Heinzinger et al. 1995).

I now examine the sulfur metabolic processes in methanogens and acetogens to understand this further, and explore how early life was forced to cope with toxic sulfite.

#### 4.4.1 Sulfite detoxification

In methanogens that inhabit sulfur rich hydrothermal environments (e.g., Takai et al. 2004), a class of enzymes are present that closely resemble *Dsr* (**Chapter 3.1**) which are used to detoxify sulfite by reducing it to sulfide. The first *Dsr-LP* to evolve was cytoplasmic and obtained electrons from intracellular Fe-S clusters which themselves would have obtained electrons from an unknown carrier (Susanti and Mukhopadhyay 2012). A later variety integrated the Fe-S clusters within the enzyme, allowing the *Dsr-LP* to obtain electrons directly from it and facilitating greater reaction rates (Susanti and Mukhopadhyay 2012). After a duplication (forming the A and B subunits; Dhillon et al. 2005), molecular analysis shows that the *DsrM* complex, which links the *DsrAB* to the electron transport chain, is homologous to the hetero-disulfide reductase enzymes (E subunit) of methanogens (Grien et al. 2013). This is also involved in the electron transport chain, which implies that the binding of the ancestral *DsrAB* complex to an *HdrE* linked it to the central energy metabolism and allowed it to act as an electron acceptor in the earliest form of respiration (Grein et al. 2013). A variety of *Dsr-LP* known as *Fsr* appears to have been convergently coupled with the *F420-H2 Dehydrogenase* enzyme (Susanti and Mukhopadhyay 2012). A variety of the derivation of *Dsr* from an enzyme utilized by methanogens to detoxify sulfite suggests that sulfur metabolism may have started out at hydrothermal vents perhaps evolved from a carbonate-reducing metabolism.

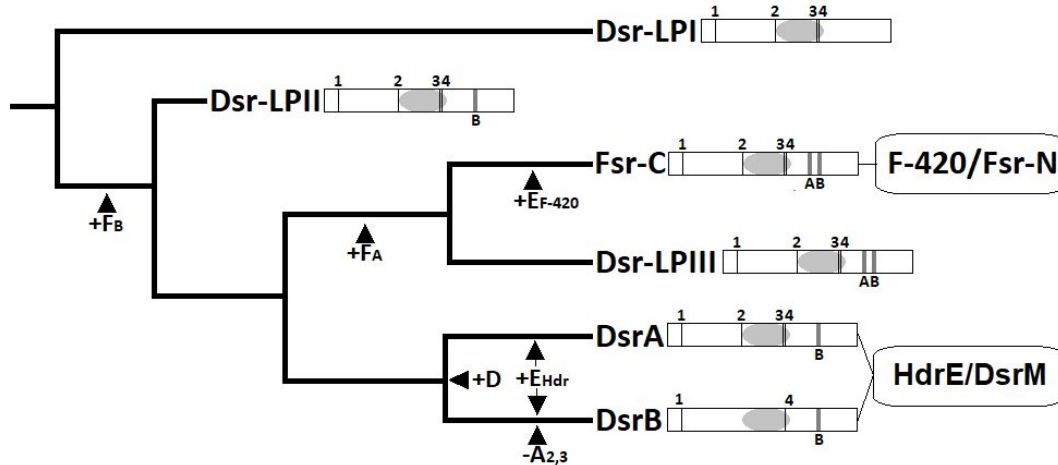


Figure 6. Position of the DsrA and DsrB subunits within the phylogeny of Dsr-like proteins in methanogens and the corresponding gene annotations. Black bands represent Arg/Lys binding sites (numbered C to N) while gray bands represent iron-sulfur clusters. F, A, D and E represent the insertion (+) or deletion (-) of an iron-sulfur cluster, Arg/Lys binding site, gene duplication or coupling of an ETC associated enzyme (adapted from Susanti and Mukhopadhyay 2012; Grein et al. 2013).

Abundant sulfite in the environment provided at least a mild selective pressure on methanogens to detoxify it. Initially, early *Dsr-LP* would have had low reaction rates but with the incorporation of sirohemes, electron transfer efficiency increased, allowing it to reduce sulfite at an increased rate (Susanti and Mukhopadhyay 2012) and inhabit deeper parts of the hydrothermal vent system with greater concentrations of  $H_2$  present (McCollum 2007). As the organisms colonized microhabitats with ever higher concentrations of sulfite, the selective pressure to detoxify it may have driven the coupling of the *Dsr-LP* to the central energy metabolism, and thus to respiration (Grein et al. 2013).

Among the many forms of sulfur respiration, sulfite reduction has some inherent limitations due to the toxicity of the substrate (Simon and Kroneck 2013). By allowing for greater metabolic rates (Widdell et al. 2013), this would have favored the evolution of sulfur respiration systems that could reduce other less-toxic oxidized sulfur compounds.

Although organisms that had evolved the capacity to reduce other sulfur sources would still have inhabited an environment where sulfite was present, the uptake of sulfite into the cytoplasm where it would do the most harm would no longer be required to carry out respiration (Dudley and Frost 1994). While sulfate was present at trace amounts, hydrolysis reactions between sulfur dioxide and calcium oxide and the reactions discussed above could also have produced sulfate in Hadean-Archean volcanic vents (Arndt and Nisbet 2012) and, when alkaline conditions are present, sulfides readily react with water to form thiosulfate (Gartman and Luther 2013). For more about reactions that yield sulfate in the pre-GOE Earth, see **Chapter 3.3.1**. The competing back-reactions to elemental sulfur can occur with oxidation of hydrogen sulfide (Luther et al. 2011) and the acid dissociation of thiosulfate (Xu et al. 1998) and polysulfide (Luther, 1990).

#### *4.4.2 Rise of sulfate, thiosulfate, tetrathionate, and elemental sulfur metabolisms*

After the first form of sulfur respiration evolved, other styles would follow suit including the ability to utilize sulfate, thiosulfate, tetrathionate and elemental sulfur/polysulfides (e.g., Duval et al. 2008). The latter three of these sulfur species are reduced by enzymes in the molybdopterin superfamily (Duval et al. 2008). Of the genes in this family likely evolved from an arsenite oxidase (*Aro*) enzyme present since before the community of LUCA (Lebrun et al. 2003). Of the sulfur species metabolized by genes in this family, the molecular structure of thiosulfate most closely resembles arsenate. Consequently, one likely scenario for the incorporation of it in sulfur metabolism is that an ancient *Aro* enzyme became attached to the end of the electron transfer chain causing it to reduce the substrate as opposed to oxidizing it and reversing

the reaction (Heinzinger et al. 1995) and bound thiosulfate to the active site. The modern *Phs* is capable of reducing compounds with a similar molecular structure to thiosulfate such as perchlorate and may be able to reduce arsenate itself (Duval et al. 2008). Due to high sequence similarity, *Phs* and *Psr/Sre* are often not distinguished from one another on phylogenies, but Melton et al. (2016) showed that when differentiated it appears that *Psr* was monophyletic while *Phs* was paraphyletic. This reinforces the notion that *Phs* represents the primitive character state of the sulfur metabolizing enzymes in the molybdopterin family. Furthermore, the *Phs*/16srDNA phylogenies are congruent across archaea and bacteria indicating that this gene was also present at LUCA (Duval et al. 2008). Presently, sulfate is most widely used in sulfur-based respiration owing to its abundance in seawater (Grein et al. 2013). Yet, the utilization of sulfate required the evolution of two other enzymes: sulfate adenylyltransferase (*Sat*) and adenylylsulfate reductase (*Apr*) (Grien et al. 2013). The *Sat* enzyme is a transferase related to kinases (Segel et al. 1987) whereas *Apr* is a reductase enzyme distantly related to other flavoproteins with a high structural but low sequence similarity (Grein et al. 2013). The phylogeny of *Apr* has a root in between sulfur reducing Archaea and group I sulfur oxidizing bacteria with sulfur oxidizing group II branching off from the sulfate reducers (Meyer and Kuever 2007). When sulfur oxidizing and sulfur reducing *Dsr* genes are placed on a phylogeny, the branches by the root are comprised of sulfur reducers with sulfur oxidizing bacteria branching off later (Müller et al. 2015). The combined *Dsr* and *Apr* gene phylogeny indicates that shortly after the ability to reduce sulfate had evolved in a stem group Archaeon, stem group

Bacteria acquired *Sat* and *Apr* via horizontal gene transfer where the pathway was reversed (Hipp et al. 1998).

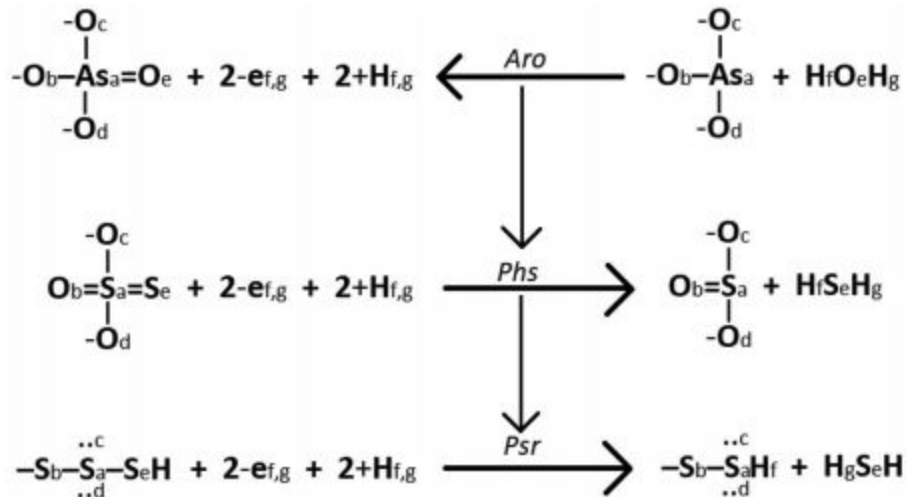


Figure 7. A proposed scenario for the evolution of the *Phs* and *Psr/Sre* enzymes. Horizontal arrows indicate the direction in which the reaction occurs whereas subscript letters by the atoms in each molecule show where a homologous site in each enzyme would interact with the products and reactants (modified from Duval et al. 2008).

#### 4.4.3 Arrival of photolithotrophy

A proposed mechanism for this reversal is when a photon struck a heme group in the electron transport chain provided an excess of energy (a product), that reversed the direction of the reaction. If this interpretation is correct, the heme group served as the precursor of the first photosynthetic pigments (bacteriochlorophyll utilized by photolithotrophs is structurally intermediate between tetrapyrroles and chlorophyll) while the protein in which it resides served as the ancestral photosystem (Martin et al. 2018). The advent of photosynthesis forever altered the stoichiometry of the global biosphere (e.g., Falkowski and Raven 2007); this newly emergent pathway would have swamped the environment with an *abundant electron acceptor*, organic carbon.

## Chapter 5. Discussion

Elemental sulfur reduction has been shown to be the oldest form of sulfur respiration for which isotopic evidence exists, yet the molecular evidence is at odds with this being the first sulfur metabolic style. Given that *Phs* occupies the branches at the root of the *Psr/Phs* gene tree (Melton et al. 2016) and has a substrate with greater similarity to that of *Aro* (Duval et al. 2008), thiosulfate reduction likely preceded it. Furthermore, *Phs* produces sulfite as a product (Rabus et al. 2013) which would have quickly built up to toxic levels in the cell if *Dsr* had not been present (Simon and Kroneck 2013) indicating that sulfite reduction in all probability preceded thiosulfate reduction. While the incorporation of the *Phs* into dissimilatory sulfur metabolism gave early respiratory organisms the precursor of the enzyme used to metabolize elemental sulfur, it was likely the incorporation of the *Sat* and *Apr* enzyme (more specifically, the pathway reversal that followed; Hipp et al. 1998) that provided the ultimate evolutionary incentive to utilize it.

### 5.1 *Straying from the alkaline vent*

Primary productivity in contemporary serpentinization hydrothermal vents is usually carbon (electron acceptor) limited (Proskurowski et al. 2008), which means that early life forms would have competed for this resource (McCollum 2007). It is interesting to note that high temperature ultra-magnesian systems – where  $H_2$  is most abundant – tend to have low oxygen fugacity and consequently relatively higher  $H_2S/SO_2$  values (Hoshyaripour et al. 2012). Arguments have been presented that such vent chemistries were relatively commonplace on the Hadean-Eoarchean Earth (Arndt and Nisbet, 2012). Any adaptation that allowed the first organisms to synthesize the

enzyme cofactors used in primary production (that catalyzed the pre-biotic synthesis of organic carbon) from more simple starting materials gave them the new ability to carry out carbon reduction in a wider array of microhabitats in the marine realm (Sojo et al. 2016). Once this threshold was breached, colonization of the water column became possible.

With a lower organic carbon to carbonate ratio than the modern biosphere (1:9 as opposed to 1:5), the Eoarchean biosphere was both puny and less productive (Schidlowski et al. 1975; Schidlowski 1982). While it has been speculated that this was due to a lower supply of nutrients (e.g., Sleep and Bird 2007), estimates of productivity have indicated that the ancient biosphere was more specifically limited by the supply of electron donors (Ward et al. 2019). In ultramafic hydrothermal systems such as Lost City (Kelley et al. 2001), primary productivity is *electron acceptor limited*. At the periphery of the vent, however, life encountered an ocean rich in bicarbonate yet relatively poor in free hydrogen. This reverses the selective pressures on an Eoarchean biosphere that strayed from the hydrothermal vents to one that goes from electron acceptor-limited to donor-limited (Ward et al. 2019). The evolution of heterotrophic processes and methanogenesis (Martin and Sousa 2016) would have also allowed those organisms to re-mineralize organic carbon produced within and around the vent to methane and carbon dioxide (Whiticar and Faber 1986).

## 5.2 Sulfur and the dawn of photothiotrophy

The most abundant form of dissimilatory sulfur reduction utilizes sulfate as the electron acceptor and accomplishes this via the Sat, Apr and Dsr pathway. Of these enzymes, *Dsr* homologs are utilized by methanogens to detoxify sulfite suggesting that



this was the first form of S-metabolism to evolve. Furthermore, the presence of the sulfur oxidizing branch of the *Dsr* phylogeny as a clade within reducing lineages (Dahl et al. 2005) coupled with the first division of the *Apr* phylogeny being between homologs of the gene used in oxidation versus reduction (Meyer & Kuever, 2007) suggests that sulfur metabolism began with reduction while the ability to oxidize sulfides came about shortly after sulfate was used as an electron<sup>-</sup> acceptor.

If sulfur oxidation originated as a result of a reversal in the sulfur respiration pathway (Hipp et al. 1997), such a switch is unlikely to have occurred when *Dsr* was the only enzyme present due to the production of toxic sulfite (Simon and Kroneck 2013).

Before photosynthesis, MSR near volcanic vents would have been limited primarily by the supply of electron donors in the system due to the high ratio of sulfur dioxide derivatives to molecular hydrogen (e.g., Nakamura and Takai 2014), except in the cases of the hottest, most magnesian and H<sub>2</sub>-rich hydrothermal centers (**Chapter 5.1**). This would have held true especially in the cooler, more oxidized periphery of the vent community because the concentration of oxidized sulfur species exceeds that of hydrogen (free or bound to a carbon) and any external source of carbon would have been fermented by methanogenesis (King 1984; Ueno et al. 2006). While most volcanic vents have a greater concentration of sulfate and sulfite than hydrogen, sulfides still dominate (Nakamura and Takai 2014). This will result in sulfur oxidation outpacing respiration if we assume that both are only using sulfur electron donors/acceptors that are derived from the vents (McCollum 2000).

I propose that the increased abundance of organic carbon as an electron donor provided an electron donor for elemental sulfur reduction to account for its

utilization by about 3.5 Ga based on the data shown in **Figure 3**, which shows a marked increase in mass-dependent fractionation. Due to the high sequence similarity between the *Psr* and *Phs* genes, relatively few mutations would have had to occur to allow the gene to reduce elemental sulfur (Duval et al. 2008), indicating that this transition could have taken place rapidly should selective pressures arise to motivate it. While the abundance of electron donors may explain why elemental sulfur was used as an electron acceptor, it should not be forgotten that elemental sulfur is in an intermediate oxidation state (Gregersen et al. 2013).

### *5.3 Elemental sulfur reduction appears in the Paleoproterozoic as opposed to other S<sup>0</sup> pathways*

The isotopic evidence in **Figure 3** hints that biological S<sup>0</sup> reduction began in the Paleoproterozoic, but are other forms of sulfur metabolism not observed at or before this time in the geochemical record? Sulfur disproportionating organisms use sulfur oxidoreductase enzymes to metabolize elemental sulfur and it is not known how this enzyme is related to others (Urich et al. 2004). This makes it difficult to understand the circumstances under which it evolved but it is known that the disproportionation of elemental sulfur must be coupled with the reduction of ferric iron to be exergonic (Thamdrup 1993). The magnetite in the oldest banded iron-formations is diagenetic from *Green Rust* (**Chapter 3.3.1**), which means that the supply of ferric iron would be limited by solubility, thus removing the evolutionary pressure to metabolize elemental sulfur.

It is documented (Franz et al. 2007) that some contemporary photolithotroph strains such as *Allochromatium vinosum* use elemental sulfur, indeed all sulfur oxidizing

microbes use elemental sulfur as an intermediate in sulfur oxidation (Gregersen et al. 2011). Yet, as shown in **Chapter 3.3.2**, the lack of isotopic evidence for elemental sulfur oxidation to sulfate until the Neoproterozoic, as indicated by the presence of sulfates with positive  $\Delta^{33}\text{S}$  values (Paris et al. 2014), suggests that the ability to oxidize elemental sulfur had not evolved until that time even if the genes were present. With the exception of a *Psr*-like gene used to oxidize sulfate to sulfite in one operational taxonomic unit (OTU) of purple sulfur bacteria, utilizing the *Dsr*, *Apr*, and *Sat* genes while lacking the *Phs* and *Psr* enzymes, makes it seem likely that the latter two were not present in the first sulfur oxidizing microbes if the pathway ended up becoming reversed (Hipp et al. 1998).

Contemporary sulfur oxidizers use the Sox multi-enzyme complex that is in the cytochrome oxidoreductase gene family, implying that unlike sulfur reducers, early sulfur oxidizers did not have an enzyme already used in sulfur metabolism that could be converted into one that oxidized elemental sulfur (Ghosh et al. 2019). Furthermore, while sulfur reducers can use sulfate bound in barite (albeit at an attenuated rate; Karanchuk et al. 2002), sulfur oxidizers cannot do the same with sulfide bound in pyrite (Rawlings et al. 1999).

Sulfur reducers living in the periphery of a volcanic vent would face electron acceptor limitation over a wide range while photolithotrophs would have a narrow band of limitation around the periphery before being subjected to complete inhibition (Rawlings et al. 1999), restricting how many photosynthetic organisms faced electron donor limitation. The first photosynthetic organisms may not have used another sulfur

source as an electron donor, or they used a different element entirely (Martin et al. 2018).

#### *5.4 The phosphorus connection and an age-old question of evolutionary biology*

The case presented here is that what drove the widespread appearance of elemental sulfur reduction in the Paleoarchean was the widespread abundance of electron acceptors relative to donors by the beginning of photosynthesis. But this raises an interesting question: why did photosynthesis began (or at least become prevalent enough to be attestable with the evidence available in the geologic record) 3.5 Ga (Olson, 2006)? Was it just because a precursor metabolism (the respiratory electron transport chain) (Martin et al. 2017) existed prior to this time or was it influenced by global events?

In the Archean as now, primary productivity can be limited by a number of factors (Kharecha et al. 2005). Today, it is usually nutrient (N, P, or Fe) limited (Cullen et al. 1992) but in the Archean eon, it has been argued that it was instead electron acceptor limited (Ward and Rasmussen, 2019). If the narrative that, at least up to the Paleoarchean, life was tied to what materials could be provided by hydrothermal vents, the stoichiometry of vent fluids can provide some insights. In volcanic vents, where the chemistry is influenced by the contact water has with magma,  $H_2 / CO_2$  and  $H_2 / (SO_4^{-2} + SO_3^{-2})$  are low enough that hydrogen would be the limiting factor behind primary productivity (<1:2 for acetogens, <1:4 for methanogens and SRMs; Kelly 2012; Nakamura and Takai 2014). Once photosynthesis began,  $H_2S$  would act as the electron donor with  $CO_2$  as the acceptor. Given the abundance of  $CO_2$  in the Archean atmosphere and oceans, it would be intuitive to think the  $H_2S$  would limit rates of

photosynthesis (Domagal-Goldman et al. 2008). However, a more detailed look at the chemistry of volcanic vents does not support this proposal. Assuming that the first phototrophs had stoichiometric nutrient requirements similar to the Redfield Ratio (C:N:P = 106:16:1) and would require 1 H<sub>2</sub>S for every 2 carbon atoms fixed, the S:P ratio would be 53 and H<sub>2</sub>S:P ratios are usually greater than 53 in volcanic vents (Kelly 2012; Cleveland and Liptzin 2007; Rogers et al. 2007).

The aforementioned information would suggest that, depending on where photosynthesis began, it may very well have been P-limited as opposed to electron donor limited. This would, of course, depend on the environment, but if there was no external source of P outside the periphery of the volcanic vent, the rate of productivity would be limited by the concentration of phosphorus species in the vent fluids (Hao et al. 2020). **Figure 8** depicts P-percent weight ratios in Archean carbonate sediments over time and, while levels remain somewhat low, there is a large spike in the maximum concentrations around 3.5 Ga. Hf isotope (Guitreau et al. 2012) and Eu rare earth element (REE) anomalies (Liou et al. 2019) also indicate that major crust forming events occurred during this time that would have brought large quantities of phosphorus to the surface. The phosphorus laden igneous rocks would then be weathered, washing large quantities of phosphorus into the ocean (Horton, 2015) thus fertilizing it and possibly driving the sudden “appearance” of photosynthesis ~3.5 Ga (Olson et al. 2006). A similar crust forming event indicated by Hf isotope systematics and Eu REE anomalies circa 3 Ga also correspond with an abrupt increase in carbonate phosphorus levels (Guitreau et al. 2012; Liou et al. 2019).

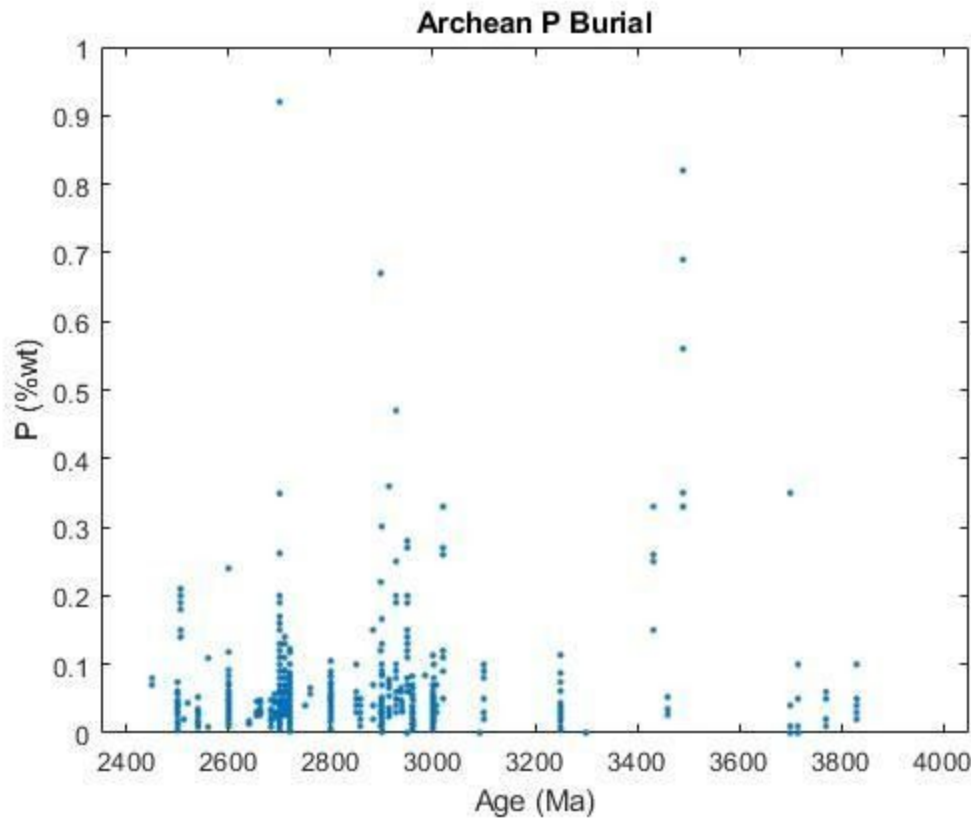


Figure 8. Concentrations of phosphorus by percent weight from Archean carbonate sediments (data obtained from other studies; link to data sheet and references in the link at the bottom).

While conclusive evidence of photosynthesis prior to 3.5 Ga remains elusive (Olson et al. 2006), the realization that the oceans became “fertilized” at this time raises the possibility that phototrophy was active pre-3.5 Ga but at levels too low to be observed due to P-limitation. If an answer to this ponderance can be identified, it may provide insight into how an age-old discussion applies to the early evolution and expansion of the planetary biosphere: gradualism versus punctuated equilibrium (Rhodes 1983). If photosynthesis appeared shortly after the Paleoproterozoic P-fertilization of the ocean took place, it would indicate that the expansion of the biosphere was driven by evolutionary innovations building upon one another (“gradualism”). Conversely, if photosynthesis began before the Paleoproterozoic crust

forming event, then it would suggest that the expansion of the biosphere was driven by sudden perturbations in the surrounding environment (“punctuated equilibrium”).

### 5.5 A Mesoarchean “iron age” of metabolism

While there was an abrupt increase in S-MDF fractionation in the Paleoarchean, there is also a relative decrease in the Mesoarchean (**Figure 3**). Although microbial S-metabolism does not drop to levels comparable to the Eoarchean, the degree of S-MIF goes below what was observed pre 3.5 Ga (**Figure 3**). If we are to ask “why was sulfur metabolism suddenly used in the Paleoarchean”, it should also be asked “why did the utilization of sulfur decrease in the Mesoarchean”. A possible explanation may be found in the limitations photoautotrophs faced post 3.5 Ga and the redox potential scale.

Photothiotrophs living on the periphery of a volcanic hydrothermal vent would have faced electron acceptor limitation with decreasing concentrations of  $\text{H}_2\text{S}$  in the primarily ferruginous Archean oceans (Crowe et al. 2014). While the zone of inhibition versus exclusion may not have been as wide for sulfate reducing microbes (discussed in **Chapter 5.3**), there would still have been selective pressures to utilize alternate sources of electron donors. One possible source was the supply of  $\text{Fe}^{2+}$  in the archean oceans itself. Today, a variety of green sulfur bacteria uses  $\text{Fe}^{2+}$  as the electron donor in photosynthesis in a process known as “photoferrotrophy” (Crowe et al. 2008). Analysis of a quaternary anoxic marine basin has indicated that photoferrotrophy (the presence of which has been indicated by green sulfur bacteria microfossils) produces hematite-rich algoma-type BIFs (Fru et al. 2013). While these are not similar to the magnetite BIFs of the Eoarchean (Nutman et al. 2017) or the superior type of the Neoproterozoic (which were most likely produced by reactions between  $\text{O}_2$  and  $\text{Fe}^{2+}$ ;

Zhang et al. 2012), there is a strong resemblance to the BIFs found in the Mesoarchean (Dai et al. 2014), suggesting biogenicity.

Although photoferrotrophy exists today, molecular analysis has indicated that the ability to utilize  $\text{Fe}^{2+}$  as an electron donor was accomplished by “coupling” an iron oxidase (*Iro*) gene utilized by  $\text{Fe}^{2+}$  oxidizing chemolithotrophs to the photosynthetic metabolism of the host green sulfur bacteria (Emerson et al 2013). This would suggest that if photoferrotrophy was occurring in the Mesoarchean, the modern ability to photo-oxidize  $\text{Fe}^{2+}$  had evolved convergently. One explanation put forth by William Martin as to how this metabolism evolved is that the  $\text{Fe}^{2+}$  was oxidized directly in the photosystem of the first photoferrotrophs. Some of these organisms later began to utilize  $\text{Mn}^{2+}$  that served as the precursor for the  $\text{CaMn}_4\text{O}_8$  cluster (the “Oxygen Evolving Complex” or OEC) used in oxygenic photosynthesis today (Martin et al. 2017; **Figure 9**). When  $\text{Mn}^{2+}$  is incorporated into the photosystem as the OEC, it is photo-oxidized to Mn(III) and Mn(IV) (Vinyard et al. 2019).



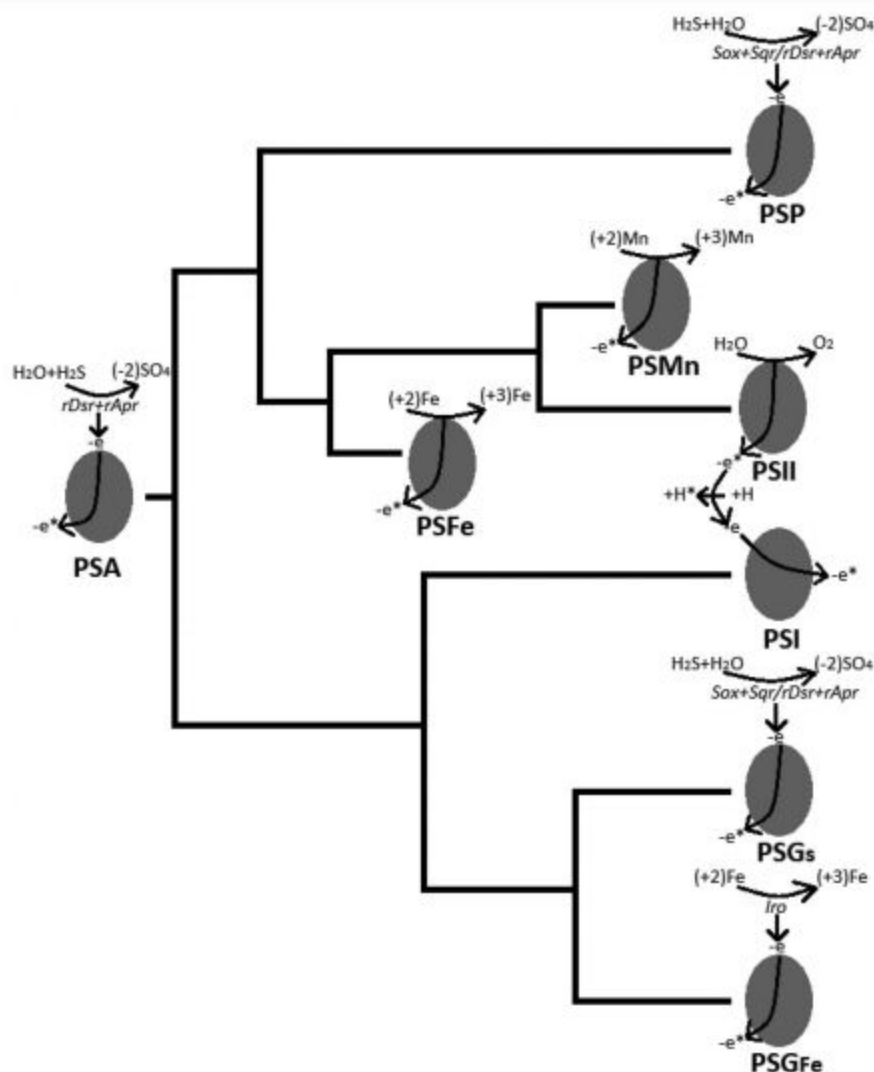


Figure 9. Possible phylogeny of the photosystems used in photosynthesis and the reaction each catalyzes with an asterisk by an electron or proton indicating that it is in a high energy state. PSA: ancestral photosystem, PSII: photosystem II, PSI: photosystem I, PSP: purple sulfur bacteria photosystem, PSGs: greens sulfur bacteria (sulfur-oxidizing) photosystem, PSGFe: greens sulfur bacteria (iron-oxidizing) photosystem, PSFe: iron-oxidizing photosystem, PSMn: manganese-oxidizing photosystem (modified from Xiong 2007; Martin et al. 2018).

Given the prevalence of  $\text{Fe}^{2+}$  in the Archean oceans (Crowe et al. 2008), photoferrotrophy could become far more abundant than phototithotrophy and it may also explain why S-MIF also decreased during the Mesoarchean (**Figure 3**). One often proposed explanation is the formation of UV-shielding organic hazes over the ocean but modeling of the mixing ratios indicated that appropriate  $\text{CH}_4/\text{CO}_2$  ratios would have

resulted in major glaciations (Domagal-Goldman et al. 2008). In the contemporary oceans, planktonic algae produce a wide variety of small volatile organic molecules that diffuse from the oceans into the atmosphere. In the phanerozoic, high  $O_2$  concentrations result in these compounds being oxidized (Halsey et al. 2017) but in the hypoxic conditions of the Mesoarchean, said volatile compounds would build up in the atmosphere and photochemical reactions with UV light could then produce a UV shielding “tholin haze” (Gudipati et al. 2013). As soon as oxygenic photosynthesis became widespread in the Neoproterozoic, the tholins would be oxidized allowing UV light to penetrate the atmosphere prior to the formation of an ozone layer resulting in greater rates of S-MIF (**Figure 3**).

If photoferrotrophy became abundant throughout the Archean oceans around 3.2 Ga, why would this result in the decreased utilization of sulfur as an electron acceptor (**Figure 3**). The presence of photoferrotrophy would provide an abundant supply of ferric iron that, like oxidized sulfur species, could be used as an electron acceptor in respiration. In fact, because the reduction of  $Fe^{3+}$  to  $Fe^{2+}$  (“Dissimilatory Iron Reduction” or “DIR”) has a greater reduction potential than  $H_2S$  to  $SO_4^{-2}$ , in systems where electron acceptors for both forms of respiration are present, DIR will outcompete MSR (Herndon et al. 2018). C-isotope analysis of Mesoarchean BIFs have suggested that DIR was present during this time (Smith et al. 2013). If these signatures are indeed indicative of DIR, it could provide an explanation for the decrease in MSR (along with the decrease in the photolytic production of  $S^0$  and  $SO_4^{-2}$ ) in the Mesoarchean. If oxygen production became widespread in the Neoproterozoic (Fakraea et al. 2018), the four eras of the Archean can be labelled by which element acted as the main electron

donor in primary productivity; the Eoarchean would represent the “hydrogen age”, the Paleoproterozoic the “sulfur age”, the Mesoproterozoic the “iron age” and the Neoproterozoic the “oxygen age”.

## 6. Conclusions

Here I have demonstrated that the expansion of microbial control of the sulfur cycle from the earliest vestiges of the geologic record can be traced by sulfur isotope geochemistry (e.g., Thiemens and Lin 2019). Prior to the evolution of the contemporary array of sophisticated sulfur metabolic styles, Earth's earliest biosphere was meager, perhaps powered mostly by the reduction of carbonates using hydrogen as the electron donor where it was locally over-abundant (e.g., Sleep and Bird 2007; Martin et al. 2016). I hypothesize that a way station for the early biosphere was in hydrogen-rich alkaline hydrothermal vents followed by inorganic carbon rich basaltic volcanic vents.

I further propose that the springboard to novel sulfur-based metabolisms at the Eoarchean to Paleoarchean transition (i.e., from ca. 3.85 Ga to 3.5 Ga) came about from sulfur reducing genes of a precursor variety used to detoxify sulfite associated with dissimilatory carbon metabolism. This would place the timing of the colonization of the volcanic vent environments to the end of the Eoarchean given that the Dsr enzyme likely existed around this time (Weiss et al. 2016, Muller et al. 2005). This idea comports well with the notion of a primordial microbial biosphere powered at some stage primarily by the reduction and fermentation of carbon (Weiss et al. 2016; Schönheit et al. 2016). This evolutionary innovation was then followed by the ability to utilize thiosulfate (Duval et al. 2008) and sulfate (Meyer and Kuever 2007) as electron acceptors. Although one question that is raised is that if the systems that the first sulfur

reducing microbes inhabited were electron donor limited, then what selective pressures drove these organisms to evolve the ability to utilize other sulfur sources? The penultimate reason that early Archean microorganisms developed the *Dsr* enzymes was because of the harmful nature of sulfite. The tendency of sulfite to break down biomolecules will still be a concern for microorganisms even if it is used as an electron acceptor. If early sulfur reducers could utilize other sources of sulfur then the quantity of sulfite uptake required to sustain respiratory processes would decrease, thus giving these organisms an advantage (Widdel and Pfennig 1981). After *Phs* had evolved from an *Aro*, the earliest sulfur reducers possessed a gene that with few modifications could use elemental sulfur as an electron acceptor (Duval et al. 2008). To induce this jump, an evolutionary pressure would likely have to be present to support the sequence of alterations to the gene required to metabolize an alternative substrate.

As part of this narrative, the excitation of electrons contained in tetrapyrrole groups of the electron transport chains by photons in the sulfate reduction pathway yielded excess energy and reversed the pathway, giving rise to the first form of photosynthesis. Others have surmised that the first forms of photosynthesis used the *Sqr* genes to oxidize sulfides to elemental sulfur (Martin et al. 2018) but the shared presence of the *Sat*, *Apr*, and *Dsr* genes in the metabolism ancestral to sulfur oxidation suggests that sulfur oxidation began with sulfate as the end product (Hipp et al. 1998).

Whereas microbial sulfur reduction within the confines of volcanic vents may have been electron donor limited (depending on vent temperature and fugacity), with the advent of the first photosynthetic organisms this situation on the periphery would have reversed this situation. Sulfur reducers in the periphery of the vent system could

use biogenic sulfate as an electron acceptor to re-mineralize organic matter (Bontognali et al. 2012), while further away from the vent, sulfate would be dropped out of the water column as insoluble barium sulfate (barite). Sulfur reducers can use sulfates bound in barites, but this happens at reduced rates compared to other sulfate sources (Karanchuk et al. 2002) resulting in MSR becoming  $e^-$  acceptor limited. This selective pressure was placed on sulfur reducers, driving the use an alternative form of sulfur (elemental sulfur) to carry out remineralization; MIF sulfur isotopes show that this was provided by atmospheric aerosols but only metabolization of this substrate began to manifest itself after the Eoarchean time (**Figure 3**).

Low temperature volcanic vents produce far more reduced sulfur than oxidized species (Nakamura and Takai 2014), which means that when utilizing volcanogenic chemicals, sulfur oxidation will outpace reduction (McCollum 2000). I hypothesize that this would result in most of the organic carbon produced by photosynthesis being emitted into the surrounding waters as opposed to being re-mineralized in the periphery of the vent accounting for the observed preference for elemental sulfur over sulfate by sulfur reducers in the multiple sulfur isotope data for the Archean.

In the ferruginous Archean oceans, lacking the ability to oxidize sulfides bound in pyrite would have contracted the threshold between limitation and complete inhibition in sulfur oxidizers, resulting in less electron donor limited primary production. This, along with the lack of precursor enzyme that could be readily adapted to metabolize elemental sulfur means that sulfur oxidizers required a greater quantity of changes while having less selective pressure than sulfur reducers to utilize elemental sulfur.

This narrative is merely one explanation for the multiple sulfur isotope patterns observed in Eo- to Paleoarchean rocks; there are many unknowns. Future work might consider a number of questions that can provide valuable insight into the expansion of the early planetary biosphere. These questions include

-What are the  $^{13}\text{C}/^{12}\text{C}$  values of organic carbon from a hydrogenotrophic organism that uses the W-L pathway and an element other than a carbon compound as the electron acceptor (Schauder et al. 1988)? Usually, the carbon that is most depleted in  $^{13}\text{C}$  fixed by methanogens and acetogens is discharged as methane or acetate because in order to meet their metabolic requirements, a greater quantity of organic carbon has to be metabolized than could possibly be assimilated. In the case of a sulfate reducer that utilized the WL-pathway, energy metabolism would be met by the sulfur-based oxidation of hydrogen so virtually all of the carbon metabolized by the WL pathway would be assimilated. Answering this question could help identify the isotopic signature of a pre photosynthetic sulfur reduction pathway.

-What changes would have to take place in the thiosulfate reductase enzyme to utilize elemental sulfur? The high sequence similarity between *Psr* and *Phs* suggest that few changes would be required (Duval et al. 2008) to occur but a detailed analysis of the active sites would be required to indicate how many amino acid substitutions had to take place (Galic et al. 2017). Although if one mutation could completely alter the gene to utilize elemental sulfur as a substrate as effectively as modern sulfur reducing organisms do, then the importance of having a selective pressure to “push” the enzyme through the incremental changes needed for an alternative substrate is attenuated and would undermine the proposed narrative.

Do sulfur reducers use any biochemical tools to metabolize barium sulfate (barite)? Many microbes use chelating factors to metabolize solid state materials (Thamdrup et al. 2000) for electron donors and acceptors. If sulfur reducers can obtain mineral-bound sulfate from barite, it would raise the possibility that such an adaptation had yet to evolve in the Paleoarchean.

- Did the biochemistry of iron metabolism evolve from sulfur metabolism, or the other way around? As comparative molecular information has indicated that sulfur metabolism evolved from methanogenesis (Grein et al. 2013; Susanti and Mukhopadhyay 2012), such approaches may be used to understand the origins of iron metabolism.

Attention ought to be directed at the timing of the appearance of photolithotrophy that I predict will be seen within the relatively under-represented geologic record from 3.75-3.5 Ga Eoarchean-Paleoarchean rocks. Specifically, a target for more detailed sampling should include sulfides of the Theespruit Formation in the Barberton Greenstone belt. It is between 3553 and 3547 Ma (Kröner et al. 1996) and composed mainly of volcanic ash with intermittent metamorphosed mudstone such as felsic schists. If rates of photosynthesis are very low because it was occurring in a phosphorus limited environment, a very real possibility is that the isotopic signal could be “drowned out” in the pool of abiogenic sulfur (Ono et al. 2007). If this is the case other methods would have to be utilized to determine if photosynthesis was indeed occurring. Because photooxidation will induce a disequilibrium between the reduced and oxidized pools of various elements, one possible approach would look for



inconsistencies between the redox state as measured by isotope fractionation (Wille et al. 2013) and the expected stoichiometry of the system.

Progress toward answering these questions would help enhance our understanding of how the early evolution of microbial metabolic systems, not just sulfur-based, can be reconciled with the Eoarchean to Paleoarchean geological record. It can also give a far better understanding as to whether the evolution and expansion of the early biosphere followed a pattern of “gradualism” with incremental evolutionary innovations building on one another or “punctuated equilibrium” where major expansion events were driven by perturbations in the global planetary geochemistry. The applications of such research go beyond the Earth as it can be used as a template to understand how life can evolve and diversify on extrasolar habitable planets as well (Nna-Mvondo and Martinez-Frias 2007).

Here, I have elucidated a major transition in the global biosphere as well as provided insight into how the method by which the majority of primary productivity (photosynthesis) on the current Earth operates began or at the very least came to prominence. In terms of developing approaches to understand the ancient biosphere for which clues are few and far between, I have illustrated how geological data, biological analysis, and information about modern analog environments can be combined to give a picture of how the biosphere evolved and expanded. Although volcanic “black smoker” vents have been replaced by serpentinizing habitats as the prime candidate for the origin of life (as environments in which the first forms of respiration and photosynthesis began), should the narrative proposed in this thesis hold out to be true, “black smoker” habitats will nonetheless hold a key position in the early

evolution of life on Earth. Overall, the content of this thesis provides a more comprehensive picture of how the ancient biosphere evolved at a metabolic level.

**References.**

- Alleon, J and Summons, R E. 2019. Organic geochemical approaches to understanding early life. *Free Radic Biol Med*, 140:103–112.
- Allwood, A C, Rosing, M T, Flannery, D T, Hurowitz, J A, Heirwegh, C M. 2018. Reassessing evidence of life in 3,700-million-year-old rocks of Greenland. *Nature*, 563:241–244.
- Arndt, N T and Nisbet, E G. 2012. Processes on the Young Earth and the Habitats of Early Life. *Ann Rev Earth Planet Sci*, 40:521–549.
- Arrhenius, G O. 2003. Crystals and life. *Helv Chim Acta* 86:1569–1586.
- Avetisyan, K, Buchshtav, T and Kamyshnyn A. 2019. Kinetics and mechanism of polysulfides formation by a reaction between hydrogen sulfide and orthorhombic elemental sulfur. *Geochim Cosmochim Acta*, 247: 96–105.
- Bak, F and Pfennig, N. 1987. Chemolithotrophic growth of *Desulfivibrio sulfodismutans* sp. nov. by disproportionation of inorganic sulfur compounds. *Archiv. Microbio.* 147: 184–189.
- Baroni, M, Thiemens, M H, Delmas, R J and Savarino, J. 2007. Mass-independent sulfur isotopic compositions in stratospheric volcanic eruptions. *Science*, 315: 84–87.
- Bekker, A, Barley, M E, Fiorentini, M L, Rouxel, O J and Rumble, D. 2009. Atmospheric sulfur in Archean komatiite-hosted nickel deposits. *Science* 326: 1086–1089.
- Bell, E A, Boehnke, P, Harrison, T M and Mao, W L. 2015. Potentially biogenic carbon preserved in a 4.1 billion-year-old zircon. *Proc Natl Acad Sci U S A*, 112: 14518–14521.
- Benner, S A, Bell, E A, Biondi, E, Brassler, R, Carell, T, Kim, H-J, Mojzsis, S J, Omran, A, Pasek, M A and Trail D. 2020. When did Life Likely Emerge on Earth in an RNA-First Process? *ChemSystemsChem*, 2: e1900035.
- Berner, R A. 1970. Sedimentary pyrite formation. *Am J Sci*, 268: 1–23.
- Berner, R A. 1984. Sedimentary pyrite formation – an update. *Geochim Cosmochim Acta*, 48: 605–615.

- Bolhar, Robert, et al. "Chemical characterization of earth's most ancient clastic metasediments from the Isua Greenstone Belt, southern West Greenland." *Geochimica et Cosmochimica Acta* 69.6 (2005): 1555-1573.
- Bontognali, T R R, Sessions, A L, Allwood, A C, Fischer, W W, Grotzinger, J P, Summons, R E and Eiler, J M. 2012. Sulfur isotopes of organic matter preserved in 3.45- billion-year-old stromatolites reveal microbial metabolism. *Proc Nat Acad Sci USA* 109: 15146–15151.
- Bottke, W. F., et al. "Dating the Moon-forming impact event with asteroidal meteorites." *Science* 348.6232 (2015): 321-323.
- Braakman, R, Smith, E. 2012. The Emergence and Early Evolution of Biological Carbon-Fixation. *PLoS Comput Biol* 8: e1002455.
- Canfield D E. 2001. Biogeochemistry of sulfur isotopes. *Rev Mineral Geochem* 43: 607–636.
- Canfield, D E and Teske, A. 1996. Late Proterozoic rise in atmospheric oxygen concentration inferred from phylogenetic and sulfur-isotope studies. *Nature* 382: 127–132.
- Canfield, D E and Thamdrup, B. 1994. The production of <sup>34</sup>S-depleted sulfide during bacterial disproportionation of elemental sulfur. *Science* 266: 1973–1975.
- Canfield, D E and Thamdrup, B. 1996. Fate of elemental sulfur in an intertidal sediment. *FEMS Microbiol Ecol*, 19: 95–103
- Canfield, D E, Thamdrup, B and Fleisher, S. 1998. Isotope fractionation and sulfur metabolism by pure and enrichment cultures of elemental sulfur-disproportionating bacteria. *Limn. Oceanol.* 43: 253–264.
- Canfield, D E. 2001. Biogeochemistry of sulfur isotopes: Stable Isotope Geochemistry. *Rev in Mineral Geochem*, 43: 607–636.
- Claire M A, Kasting, J F, Domagal-Goldman, S D, Stüeken, E E, Buick, R and Meadows, V S. 2014. Modeling the signature of sulfur mass-independent fractionation produced in the Archean atmosphere. *Geochim Cosmochim Acta*, 141: 365–380.
- Claypool, G E and Mancini, E A. 1989. Geochemical relationships of petroleum in Mesozoic reservoirs to carbonate source rocks of Jurassic Smackover

- Formation, southwestern Alabama. *Amer Assoc Petroleum Geol Bull*, 73: 904–924.
- Cleveland, Cory C., and Daniel Liptzin. "C: N: P stoichiometry in soil: is there a "Redfield ratio" for the microbial biomass?." *Biogeochemistry* 85.3 (2007): 235-252.
- Craddock, Paul R., et al. "Sulfur isotope measurement of sulfate and sulfide by high-resolution MC-ICP-MS." *Chemical Geology* 253.3-4 (2008): 102-113.
- Crowe, Sean A., et al. "Photoferrotrophs thrive in an Archean Ocean analogue." *Proceedings of the National Academy of Sciences* 105.41 (2008): 15938-15943.
- Crowe, S A, Paris, G, Katsev, S, Jones, C, Kim, S-T, Zerkle, A L, Nomosatryo, S, Fowle, D A, Adkins, J F, Sessions, A L, Farquhar, J and Canfield, D E. 2014. Sulfate was a trace constituent of Archean seawater. *Science* 346: 735–739.
- Cullen, John J., Xiaolong Yang, and Hugh L. MacIntyre. "Nutrient limitation of marine photosynthesis." *Primary productivity and biogeochemical cycles in the sea*. Springer, Boston, MA, 1992. 69-88.
- Cypionka, H., Smock, A M and Bottcher, M E. 1998. A combined pathway of sulfur compound disproportionation in *Desulfovivrio desulfuricans*. *FEMS Microbio Lett*, 166: 181–186.
- Dahl, Christiane, et al. "Novel genes of the *dsr* gene cluster and evidence for close interaction of Dsr proteins during sulfur oxidation in the phototrophic sulfur bacterium *Allochromatium vinosum*." *Journal of bacteriology* 187.4 (2005): 1392-1404.
- Dahl C. 2017. Sulfur metabolism in phototrophic bacteria. In: Hallenbeck PC (ed.). *Modern Topics in the Phototrophic Prokaryotes*. Cham: Springer International 27–66.
- Dai, Yanpei, et al. "The composition and genesis of the Mesoarchean Dagushan banded iron formation (BIF) in the Anshan area of the North China Craton." *Ore Geology Reviews* 63 (2014): 353-373.
- Dhillon, A, Goswami, S, Riley, M, Teske, A and Sogin, M. 2005. Domain evolution and functional diversification of sulfite reductases. *Astrobio*, 5: 18–29.

- Ding, T, Valkiers, S, Kipphardt, H, DeBièvre, P, Taylor, P D P, Gonfiantini, R and Krouse, R. 2001. Calibrated sulfur isotope abundance ratios of three IAEA sulfur isotope reference materials and V-CDT with reassessment of the atomic weight of sulfur. *Geochim Cosmochim Acta* 65: 2433–2437.
- Dodd, M S, Papineau, D, Grenne, T, Slack, J F, Rittner, M, Pirajno, F, O’Neil, J and Little, C T S. 2017. Evidence for early life in Earth’s oldest hydrothermal vent precipitates. *Nature*, 543: 60–64.
- Domagal-Goldman, S, Poirier, B and Wing, B. 2011. Mass-independent fractionation of sulfur isotopes: Carriers and Sources. Summary Report of NASA Workshop, 36 p.
- Domagal-Goldman, Shawn D., et al. "Organic haze, glaciations and multiple sulfur isotopes in the Mid-Archean Era." *Earth and Planetary Science Letters* 269.1-2 (2008): 29-40.
- Dudley, M W and Frost, J W. 1994. Biocatalytic desulfurization of arylsulfonates. *Bioorg Med Chem*, 2: 681–690.
- Duval, S, Ducluzeau, A-L, Nitschke, W and Schoepp-Cothenet, B. 2008. Enzyme phylogenies as markers for the oxidation state of the environment: the case of respiratory arsenate reductase and related enzymes." *BMC evolutionary biology* 8: 206.
- Eickmann, B, Hofmann, A, Wille, M, Bui, T H, Wing, B A and Schoenberg, R. 2018. Isotopic evidence for oxygenated Mesoarchean shallow oceans. *Nature Geosci*, 11: 133–138.
- Emerson, David, et al. "Comparative genomics of freshwater Fe-oxidizing bacteria: implications for physiology, ecology, and systematics." *Frontiers in microbiology* 4 (2013): 254.
- Fakhraee, Mojtaba, Sean A. Crowe, and Sergei Katsev. "Sedimentary sulfur isotopes and Neoproterozoic ocean oxygenation." *Science advances* 4.1 (2018): e1701835.
- Falkowski, P G. 2006. Evolution. Tracing oxygen's imprint on earth's metabolic evolution. *Science*. 311: 1724–1725.

Falkowski, P G and Raven, J A. 2007. Aquatic Photosynthesis. Princeton University Press, 484 p.

- Farquhar, J and Wing, B A. 2003. Multiple sulfur isotopes and the evolution of the atmosphere. *Earth Planet Sci Lett*, 213: 1–13.
- Farquhar, J, Bao, H and Thiemens, M. 2000. Atmospheric influence of Earth's earliest sulfur cycle. *Science*, 289:756–759.
- Farquhar, J, Johnston, D T, Wing, B A, Habicht, K S, Canfield, D E, Airieau, S and Thiemens M H. 2003. Multiple sulphur isotopic interpretations of biosynthetic pathways: implications for biological signatures in the sulphur isotope record. *Geobiology*, 1: 27–36.
- Farquhar, J, Savarino, J, Airieau, S and Thiemens, M H. 2001. Observation of wavelength-sensitive mass-independent sulfur isotope effects during SO<sub>2</sub> photolysis: Implications for the early atmosphere. *J Geophys Res*, 106: 32829–32839.
- Fike, D A and Grotzinger, JP. 2008. A paired sulfate–pyrite  $\delta^{34}\text{S}$  approach to understanding the evolution of the Ediacaran-Cambrian sulfur cycle. *Geochim. Cosmochim. Acta* 72:2636–2648.
- Fike, D A, Bradley, A S and Rose, C V. 2014. Rethinking the ancient sulfur cycle. *Annu Rev Earth Planet Sci*, 43:593–622.
- Fike, D A, Grotzinger, J P, Pratt, L M and Summons, R E. 2006. Oxidation of the Ediacaran ocean. *Nature* 444:744–747.
- Finster, K, Liesack, W and Thamdrup, B. 1998. Elemental sulfur and thiosulfate disproportionation by *Desulfocapsa sulfoexigens* sp. nov., a new anaerobic bacterium isolated from marine surface sediment. *Appl. Environ. Microbio.* 64: 119–125.
- Franz, B, Lichtenberg, H, Hormes, J, Modrow, H, Dahl, C and Prange, A. 2007. Utilization of solid "elemental" sulfur by the phototrophic purple sulfur bacterium *Allochromatium vinosum*: A sulfur K-edge XANES spectroscopy study. *Microbiol* 153: 1268–1274.
- Fru, Ernest Chi, et al. "Fossilized iron bacteria reveal a pathway to the biological origin of banded iron formation." *Nature communications* 4.1 (2013): 1-7.



- Galić, A, Mason, P R D, Mogollón, J M, Wolthers, M, Vroon, P Z and Whitehouse, M J. 2017. Pyrite in a sulfate-poor Paleoproterozoic basin was derived predominantly from elemental sulfur: evidence from 3.2 Ga sediments in the Barberton Greenstone Belt, Kaapvaal Craton. *Chem Geol*, 449: 135–146.
- Gartman, A and Luther III, G W. 2013. Comparison of pyrite ( $\text{FeS}_2$ ) synthesis mechanisms to reproduce natural  $\text{FeS}_2$  nanoparticles found at hydrothermal vents. *Geochim Cosmochim Acta* 120: 447–458.
- Génin, J-M R, Bourrié, G, Trolard, F, Abdelmoula, M, Jaffrezic, A, Refait, P, Maitre, V, Humbert, B and Herbillon, A. 1998. Thermodynamic Equilibria in Aqueous Suspensions of Synthetic and Natural Fe(II)–Fe(III) Green Rusts: Occurrences of the Mineral in Hydromorphic Soils. *Environ Sci Tech*, 32: 1058–1068.
- Ghosh, W, Mallick, S and DasGupta, S K. 2009. Origin of the Sox multienzyme complex system in ancient thermophilic bacteria and coevolution of its constituent proteins. *Res Microbiol* 160: 409–420.
- Gill, B C, Lyons, T W, Young, S A, Kump, L R, Knoll, A H and Saltzman M R. 2011. Geochemical evidence for widespread euxinia in the Later Cambrian ocean. *Nature* 469:80–83.
- Goldford, J E., Hartman, H, Marsland III, R and Segrè, D. 2019. Environmental boundary conditions for the origin of life converge to an organo-sulfur metabolism. *Nature Ecol Evol* 3: 1715–1724.
- Goldhaber, M B and Kaplan, I R. 1975. Controls and consequences of sulfate reduction rates in recent marine sediments. *Soil Sci*, 119: 42–55.
- Greer, J C, Cates, N L, Caro, G, Bleeker, W, Kelly, N M and Mojzsis, S J. 2020. Polyphase Archean granitoid gneisses and supracrustal enclaves of the southern Inukjuak Domain, Quebec (Canada). *Lithos*, 364–365: 105520.
- Gregersen, L H, Bryant, D A and Frigaard, N-U. Mechanisms and evolution of oxidative sulfur metabolism in green sulfur bacteria. *Front Microbio* 2: 116.
- Grein, F, Ramos, A R, Venceslau, S S and Pereira, I A C. 2013. Unifying concepts in anaerobic respiration: insights from dissimilatory sulfur metabolism. *Biochim Biophys Acta*, 1827:145–160.

- Gudipati, Murthy S., et al. "Photochemical activity of Titan's low-altitude condensed haze." *Nature communications* 4.1 (2013): 1-8.
- Guitreau, Martin, et al. "Hafnium isotope evidence from Archean granitic rocks for deep-mantle origin of continental crust." *Earth and Planetary Science Letters* 337 (2012): 211-223.
- Gutzmer, J., et al. "The origin and paleoenvironmental significance of stratabound barites from the Mesoarchean Fig Tree Group, Barberton Mountainland, South Africa." *SSAGI-V South America Symposium on isotope geology (24–27 April 2006), Abstract Volume*. Vol. 311. 2006.
- Guy, B M, Ono, S, Gutzmer, J, Lin, Y, Fogel, M L and Beukes, N J. 2012. A multiple sulfur and inorganic carbon isotope record from non-conglomeratic sedimentary rocks of the Mesoarchean Witwatersrand Supergroup, South Africa. *Precamb Res*, 219: 208–231.
- Habicht, K S, Canfield, D E and Rethmeier, J. 1998. Sulfur isotope fractionation during bacterial reduction and disproportionation of thiosulfate and sulfite. *Geochim Cosmochim Acta* 62: 2585–2595.
- Habicht, K S, Gade, M, Thamdrup, B, Berg, P and Canfield, D E. 2002. Calibration of sulfate levels in the Archean ocean. *Science* 298:2372–2374.
- Halevy, I, Alesker, M, Schuster, E M, Popovitz-Biro, R and Feldman, Y. 2017. A key role for green rust in the Precambrian oceans and the genesis of iron formations. *Nature Geosci* 10:135–139.
- Hao, Jihua, et al. "Cycling phosphorus on the Archean Earth: Part II. Phosphorus limitation on primary production in Archean ecosystems." *Geochimica et Cosmochimica Acta* (2020).
- Harrison, A G and Thode, H G. 1958. Mechanisms of bacterial reduction of sulfate from isotope fractionation studies. *Trans Faraday Soc*, 53: 84–92.
- Hattori, K and Cameron, E M. 1986. Archaean magmatic sulphate. *Nature*, 319: 45–47.
- Hattori, K and Cabri, L J. 1992. Origin of platinum-group mineral nuggets inferred from an Osmium-isotope study. *Canadian Mineral*, 30: 289–301.

- Hattori S, Schmidt, J A, Johnson, M S, Danielache, S O, Yamada, A, Ueno, Y and Yoshida, N. 2013. SO<sub>2</sub> photoexcitation mechanism links mass-independent sulfur isotopic fractionation in cryospheric sulfate to climate impacting volcanism. *Proc Natl Acad Sci USA*, 110:17656–17661.
- Havig, J R, Hamilton, T L, Bachan, A and Kump, L R. 2017. Sulfur and carbon isotopic evidence for metabolic pathway evolution and a four-stepped Earth system progression across the Archean and Paleoproterozoic. *Earth-Science Rev* 174: 1–21.
- Heinzinger, N K, Fujimoto, S Y, Clark, M A, Moreno, M S and Barrett, E L. 1995. Sequence analysis of the *p<sub>hs</sub>* operon in *Salmonella typhimurium* and the contribution of thiosulfate reduction to anaerobic energy metabolism. *J Bacteriol* 177: 2813–2820.
- Herndon, Elizabeth M., et al. "Manganese and iron geochemistry in sediments underlying the redox-stratified Fayetteville Green Lake." *Geochimica et Cosmochimica Acta* 231 (2018): 50-63.
- Hipp, W M, Pott, A S, Thum-Schmitz, N, Faath, I, Dahl, C and Trüper H G. 1997. Towards the phylogeny of APS reductases and sirohaem sulfite reductases in sulfate-reducing and sulfur-oxidizing prokaryotes. *Microbiol* 143: 2891–2902.
- Halsey, Kimberly H., et al. "Biological cycling of volatile organic carbon by phytoplankton and bacterioplankton." *Limnology and Oceanography* 62.6 (2017): 2650-2661.
- Holland, H D. 1973. The oceans: a possible source of iron in iron-formations. *Econ Geol*, 68: 1169–1172.
- Holland, H D. 2006. The oxygenation of the atmosphere and oceans. *Phil Trans R Soc B London*, 361:903–915.
- Holland, H D. 1984. The chemical evolution of the atmospheres and oceans. Princeton Series in Geochemistry, Princeton, pp. 598.
- Holliday, G L, Thornton, J M, Marquet, A, Smith, A G, Rébeillé, F, Mendel, R, Schubert, H L, Lawrence, A D and Warre, M J. 2007. Evolution of enzymes and pathways for the biosynthesis of cofactors. *Nat Prod Rep* 24: 972–987.

- Horton, Forrest. "Did phosphorus derived from the weathering of large igneous provinces fertilize the Neoproterozoic ocean?." *Geochemistry, Geophysics, Geosystems* 16.6 (2015): 1723-1738.
- Hoshyaripour, G, Hort, M and Langmann, B. 2012. How does the hot core of a volcanic plume control the sulfur speciation in volcanic emission? *Geochem Geophys Geosys* 13. Q07004, doi:10.1029/2011GC004020.
- Hulston J R and Thode, H G. 1965. Variations in the  $S^{33}$ ,  $S^{34}$  and  $S^{36}$  contents of meteorites and their relation to chemical and nuclear effects. *J Geophys Res* 70: 3475–3484.
- Izon G, Zerkle, A L, Zhelenskaia, I, Farquhar, J, Newton, R J, Poulton, S W, Eigenbrode, J L and Claire, M W. 2015. Multiple oscillations in Neoproterozoic atmospheric chemistry. *Earth Planet Sci Lett*, 431: 264–273.
- J Gen Microbiol*, 34: 195-212.
- Jacobsen, S B and Pimentel-Close, M R. 1988. Nd isotopic variations in Precambrian banded iron formations. *Geophys Res Lett*, 15: 393–396.
- James, H L. 1954. Sedimentary facies of iron-formation. *Econ Geol*, 49: 236–294.
- Jamieson, J W, Wing, B A, Farquhar, J and Hannington, M D. 2013. Neoproterozoic seawater sulphate concentrations from sulphur isotopes in massive sulphide ore. *Nature Geosci.* 6: 61–64.
- Jamieson, J W, Wing, B A, Hannington, M D and Farquhar, J. 2006. Evaluating isotopic equilibrium among sulphide mineral pairs in Archean ore deposits: Case study from the Kidd Creek VMS deposit, Ontario, Canada. *Econ Geol*, 101: 1055–1061.
- Janecky, D R and Shanks, W C. 1988. Computational modelling of chemical and sulfur isotope reactions processes in seafloor hydrothermal systems: Chimneys, massive sulfides and subjacent alteration zones. *Canadian Mineral*, 26: 805–825.
- Johnston, D T, Farquhar, J, Wing, B A, Kaufman, A, Canfield, D E and Habicht, K S. 2005. Multiple sulfur isotope fractionations in biological systems: a case study with sulfate reducers and sulfur disproportionators. *Am J Sci*, 305: 645–660.

- Johnston, D T, Farquhar, J, Wing, B A, Kaufman, A, Canfield, D E and Habicht, K S. 2005. Multiple sulfur isotope fractionations in biological systems: a case study with sulfate reducers and sulfur disproportionators. *Am J Sci*, 305: 645–660.
- Johnston, D T. 2011. Multiple sulfur isotopes and the evolution of Earth's surface sulfur cycle. *Earth-Science Rev*, 106:161–183.
- Jones, G E and Starkey, R J. 1957. Fractionation of isotopes of sulfur by micro-organisms and their role in the deposition of native sulfur. *J Appl Env Microbiol* 5: 111–115.
- Jørgensen, B B, Zawacki, L X and Jannasch, H W. 1990 Thermophilic bacterial sulfate reduction in deep-sea sediments at the Guaymas Basin hydrothermal vent site. *Deep-sea Res*, 37: 695–710.
- Kafantaris, F-C A and Druschel, G K. 2020. Kinetics of the nucleophilic dissolution of hydrophobic and hydrophilic elemental sulfur sols by sulfide. *Geochim Cosmochim Acta*, 269: 554–565.
- Kamber, B S, Whitehouse, M J. 2007. Micro-scale sulphur isotope evidence for sulphur cycling in the late Archean shallow ocean. *Geobiology* 5: 5–17.
- Kamyshny, A, Goifman, A, Rizkov, D and Lev O. 2003. Kinetics of disproportionation of inorganic polysulfides in undersaturated aqueous solutions at environmentally relevant conditions. *Aquat Geochem*, 9: 291–304.
- Kaplan, I R and Rittenberg. 1962. Microbiological fractionation of sulphur isotopes
- Kappler, A, Pasquero, C, Konhauser, K O and Newman, D K. 2005. Deposition of banded iron formations by anoxygenic phototrophic Fe(II)-oxidizing bacteria. *Geology*, 33: 865–868.
- Karnachuk, O, Kurochkina, S and Tuovinen, O. 2002. Growth of sulfate-reducing bacteria with solid-phase electron acceptors. *Appl Microbiol Biotech* 58: 482–486.
- Kaufman, A J, Johnston, D T, Farquhar, J, Masterson, A L, Lyons, T W, Bates, S, Anbar, A D, Arnold, G L, Garvin, J and Buick R. 2007. Late Archean biospheric oxygenation and atmospheric evolution. *Science*, 317: 1900–1903.
- Kelly, D. Energetics of chemolithotrophs. Academic Press, San Diego, 2012.

- Kharecha, P., James Kasting, and J. Siefert. "A coupled atmosphere–ecosystem model of the early Archean Earth." *Geobiology* 3.2 (2005): 53-76.
- King, G M. 1984. Utilization of hydrogen, acetate, and "noncompetitive"; substrates by methanogenic bacteria in marine sediments. *Geomicrobiol J*, 3: 275–306.
- Kiyosu, Y. 1980. Chemical reduction and sulfur isotope effects of sulfate by organic matter under hydrothermal conditions. *Chem Geol* 30: 47–56.
- Klein, C. 2005. Some Precambrian Banded Iron Formations (BIFs) from around the world: their age, geologic setting, mineralogy, metamorphism, geochemistry, and origin. *Am. Mineral*, 90: 1473–1499.
- Konhauser, K O, Lalonde, S, Amskold, L and Holland, H D. 2007. Was there really an Archean phosphate crisis? *Science*, 315: 1234.
- Krapež B, Barley, M E and Pickard, A L. 2003. Hydrothermal and resedimented origins of the precursor sediments to banded iron formation: sedimentological evidence from the Early Paleoproterozoic Brockman Supersequence of Western Australia. *Sedimentology*, 50: 979–1011.
- Kröner, A, Hegner, E, Wendt, J I and Byerly, G R. 1996. The oldest part of the Barberton granitoid-greenstone terrain, South Africa: evidence for crust formation between 3.5 and 3.7 Ga. *Precamb Res*, 78: 105–124.
- Kuma, K, Paplawsky, W, Gedulin, B and Arrhenius, G. 1989. Mixed-valence hydroxides as bioorganic host minerals. *Origin Life Evol Biosph*, 19: 573–602.
- Kumar, M and Francisco, J S. 2017. Elemental sulfur aerosol-forming mechanism. *Proc Nat Acad Sci USA*, 114: 864–869.
- Lasaga, A C, Otake, T, Watanabe, Y and Ohmoto, H. 2008. Anomalous fractionation of sulfur isotopes during heterogeneous reactions. *Earth Planet Sci Lett.*, 268: 225–238.
- Laska, S, Lottspeich, F and Kletzin, A. Membrane-bound hydrogenase and sulfur reductase of the hyperthermophilic and acidophilic archaeon *Acidianus ambivalens*. *Microbiol*, 149: 2357–2371.
- Lebrun, E, Brugna, M, Baymann, F, Muller, D, Lièvreumont, D, Lett, M-C and Nitschke, W. 2003. Arsenite oxidase, an ancient bioenergetic enzyme. *Mol Bio Evol*, 20: 686–693.

- Ledevin, Morgane, et al. "The sedimentary origin of black and white banded cherts of the Buck Reef, Barberton, South Africa." *Geosciences* 9.10 (2019): 424.
- Lepland, Aivo, and Martin J. Whitehouse. "Metamorphic alteration, mineral paragenesis and geochemical re-equilibration of early Archean quartz–amphibole–pyroxene gneiss from Akilia, Southwest Greenland." *International Journal of Earth Sciences* 100.1 (2011): 1-22.
- Liou, Peng, and Jinghui Guo. "Generation of Archaean TTG gneisses through amphibole-dominated fractionation." *Journal of Geophysical Research: Solid Earth* 124.4 (2019): 3605-3619.
- Luther III, G Q. 1990. The frontier molecular-orbital theory approach in geochemical processes. In, W. Stumm (Ed.), *Aquatic Chemical Kinetics*, John Wiley & Sons, New York, pp. 173–198.
- Luther III, G Q, Findlay, A J, MacDonald, D J, Owings, S M, Hanson, T E, Beinart, R A and Girguis, P R. 2011. Thermodynamics and kinetics of sulfide oxidation by oxygen: a look at inorganically controlled reactions and biologically mediated processes in the environment. *Front Microbiol*, 2: 62.
- Lyons J R. 2009. Atmospherically-derived mass-independent sulfur isotope signature, and incorporation into sediments. *Chem Geol*, 267:164–174.
- Lyons, T W, Reinhard, C T and Planavsky, N J. 2014. The rise of oxygen in Earth's early ocean and atmosphere. *Nature*, 506: 307–315.
- Machel, H G. 1998. Gas souring by thermochemical sulfate reduction at 140°C: Discussion. *Amer Assoc Petroleum Geol Bull*, 82: 1870–1873.
- Maier, R M. 2015. Chapter 16 – Biogeochemical Cycling. *Environmental Microbiology* (Third edition), pp. 339–373.
- Martin, W F. 2016. Physiology, phylogeny and the energetic roots of life. *Period Biol* 118: 343–352.
- Martin, W F and Russell, M J. 2007. On the origin of biochemistry at an alkaline hydrothermal vent. *Philos Trans R Soc Lond B Biol Sci* 362: 1887–1925.
- Martin, W F and Sousa, F L. 2016. Early microbial evolution: the age of anaerobes. *Cold Spring Harbor Persp Biol* 8: a018127.

- Martin, W F, Bryant, D A and Beatty, J T. 2018. A physiological perspective on the origin and evolution of photosynthesis. *FEMS Microbiol Rev* 42: 205–231.
- McCollom, T M. 2000. Geochemical constraints on primary productivity in submarine hydrothermal vent plumes. *Deep Sea Res, Part I: Oceanographic Research Papers*, 47: 85–101.
- McCollom, T M. 2007. Geochemical constraints on sources of metabolic energy for chemolithoautotrophy in ultramafic-hosted deep-sea hydrothermal systems. *Astrobio*, 7: 933–950.
- Melton, E D, Sorokin, D Y, Overmars, L, Chertkov, O, Clum, A, Pillay, M, Ivanova, N, Shapiro, N, Kyrpides, N C, Woyke, W, Lapidus, A L and Gerard Muyzer, G. 2016. Complete genome sequence of *Desulfurivibrio alkaliphilus* strain AHT2 T, a haloalkaliphilic sulfidogen from Egyptian hypersaline alkaline lakes. *Stand Genom Sci*, 11: 67.
- Meyer, B and Kuever, J. Molecular analysis of the distribution and phylogeny of dissimilatory adenosine-5'-phosphosulfate reductase-encoding genes (*aprBA*) among sulfur-oxidizing prokaryotes. *Microbiol*, 153: 3478–3498.
- Mojzsis, S J, Coath, C D, Greenwood, J P, McKeegan, K D and Harrison, T M. 2003. Mass independent isotope effects in Archean (2.5 to 3.8 Ga) sedimentary sulfides determined by ion microprobe analysis. *Geochim. Cosmochim. Acta* 67:1635–1658.
- Mojzsis, S J. 2007. Sulphur on the Early Earth. *Developments Precamb Geol*, 15: 923–970.
- Mojzsis, SJ, Arrhenius, G, McKeegan, K D, Harrison, T M, Nutman, A P and Friend, C R L. 1996. Evidence for life on Earth before 3,800 million years ago. *Nature*, 384: 55–59.
- Monster, J, Appel, P W U, Thode, H G, Schidlowski, M, Carmichael, C M and Bridgwater, D. 1979. Sulfur isotop studies in Early Archean sediments from Isua, West Greenland: implications for the antiquity of bacterial sulfate reduction. *Geochim Cosmochim Acta*, 43: 405–413.
- Morita, R Y. 2000. Is H<sub>2</sub> the universal energy source for long-term survival? *Microb Ecol*, 38: 307–320.



- Muller, Élodie, et al. "Multiple sulfur-isotope signatures in Archean sulfates and their implications for the chemistry and dynamics of the early atmosphere." *Proceedings of the National Academy of Sciences* 113.27 (2016): 7432-7437.
- Müller, A L, Kjeldsen, K U, Rattei, T, Pester, M and Loy, A. 2015. Phylogenetic and environmental diversity of DsrAB-type dissimilatory (bi)sulfite reductases. *The ISME journal* 9: 1152–1165.
- Nakamura, K, and Takai, K. 2014. Theoretical constraints of physical and chemical properties of hydrothermal fluids on variations in chemolithotrophic microbial communities in seafloor hydrothermal systems. *Progress in Earth and Planetary Science* 1: 5.
- Newton, R C and Manning, C M. 2005. Solubility of Anhydrite,  $\text{CaSO}_4$ , in  $\text{NaCl-H}_2\text{O}$  solutions at high pressures and temperatures: Applications to fluid-rock interaction. *J Petrol*, 46: 701–716.
- Nitschke, W and Russell, M J. 2013. Beating the acetyl coenzyme-A pathway to the origin of life. *Philos Trans R Soc Lond B Biol Sci* 368, 20120258.
- Nna-Mvondo, Delphine, and Jesus Martinez-Frias. "Review komatiites: from Earth's geological settings to planetary and astrobiological contexts." *Earth, moon, and planets* 100.3-4 (2007): 157-179.
- Nutman, A P, Bennett, V C, Friend, C R L, Van Kranendonk, M J and Chivas, A R. 2016. Rapid emergence of life shown by discovery of 3,700-million-year-old microbial structures. *Nature*, 537: 535–538.
- Nutman, Allen P., Vickie C. Bennett, and Clark RL Friend. "Seeing through the magnetite: Reassessing Eoarchean atmosphere composition from Isua (Greenland)≥ 3.7 Ga banded iron formations." *Geoscience Frontiers* 8.6 (2017): 1233-1240.
- Olson, J M. 2006. Photosynthesis in the Archean era. *Photosynth Res* 88: 109–117.
- O'Neil, Jonathan, et al. "Formation age and metamorphic history of the Nuvvuagittuq Greenstone Belt." *Precambrian Research* 220 (2012): 23-44.

- Ono, S, Eigenbrode, J L, Pavlov, A A, Kharecha, P, Rumble, D, Kasting, J F and Freeman, K H. 2003. New insights into Archean sulfur cycle from mass-independent sulfur isotope records from the Hamersley Basin, Australia. *Earth Planet Sci Lett*, 213: 15–30.
- Ono, S, Wing, B, Johnston, D, Farquhar, J and Rumble, D. 2006. Mass-dependent fractionation of quadruple stable sulfur isotope system as a new tracer of sulfur biogeochemical cycles. *Geochim Cosmochim Acta*, 70: 2238–2252.
- Ono, Shuhei, et al. "S-33 constraints on the seawater sulfate contribution in modern seafloor hydrothermal vent sulfides." *Geochimica et Cosmochimica Acta* 71.5 (2007): 1170-1182.
- Ono S, Whitehill, A R and Lyons, J R. 2013. Contribution of isotopologue self-shielding to sulfur mass independent fractionation during sulfur dioxide photolysis. *J Geophys Res*, 118:2444–2454.
- Orsi, W D, Schink, B, Buckel, W and Martin, W F. 2020. Physiological limits to life in anoxic subseafloor sediment. *FEMS Microbiol Rev* 44: 219-231.
- Pace, N. 2006. Time for a change. *Nature* 441, 289.
- Papineau, D, De Gregorio, B T, Cody, G D, Fries, M D, Mojzsis, S J, Steele, A, Rhonda M. Stroud, R M and Fogel, M L. 2010. Ancient graphite in the Eoarchean quartz-pyroxene rocks from Akilia in southern West Greenland II: Isotopic and chemical compositions and comparison with Paleoproterozoic banded iron formations. *Geochim Cosmochim Acta* 74: 5884–5905.
- Papineau, D, Mojzsis, S J and Schmitt, A K. 2007 Multiple sulfur isotopes from Paleoproterozoic Huronian interglacial sediments and the rise of atmospheric oxygen. *Earth Planet Sci Lett*, 255: 188–212.
- Papineau, D, Mojzsis, S J, Coath, C D, Karhu, J A and McKeegan, K D. 2005. Multiple sulfur isotopes of sulfides from sediments in the aftermath of Paleoproterozoic glaciations. *Geochim Cosmochim Acta*, 69: 5033–5060.
- Pavlov, A A and Kasting, J F. 2002. Mass-independent fractionation of sulfur isotopes in Archean sediments: strong evidence for an anoxic Archean atmosphere. *Astrobiology*, 2: 27–41.

- Philippot, P, Va Zuilen, M, Lepot, K, Thomazo, C, Farquhar, J and Van Kranendonk, M J. 2007. Early Archaean microorganisms preferred elemental sulfur, not sulfate. *Science*, 317:1534–1537.
- Philippot, P, Van Zuilen, M and Rollion-Bard, C. 2012. Variations in atmospheric sulphur chemistry on early Earth linked to volcanic activity. *Nat Geosci* 5:668–674.
- Polat, Ali, et al. "Contrasting geochemical patterns in the 3.7–3.8 Ga pillow basalt cores and rims, Isua greenstone belt, Southwest Greenland: implications for postmagmatic alteration processes." *Geochimica et Cosmochimica Acta* 67.3 (2003): 441-457.
- Posth, N R, Konhauser, K O and Kappler, A. 2013. Microbial processes in banded iron formation deposition. *Sedimentology* 60: 1733–1754.
- Preiner, M, Igarashi, K, Muchowska, K B, Yu, M, Varma, S J, Kleinermanns, K, Nobu, M K, Kamagata, Y, Tüysüz, H, Moran, J and Martin, W F. 2020. A hydrogen dependent geochemical analogue of primordial carbon and energy metabolism. *Nature Ecol Evol* 4: 534–542.
- Proskurowski, G, Lilley, M D, Seewald, J S, Früh-Green, G L, Olson, E J, Lupton, J E, Sylva, S P and Kelley, D S. 2008. Abiogenic hydrocarbon production at Lost City hydrothermal field. *Science* 319: 604–607.
- Proskurowski, G, Lilley, M D, Seewald, J S, Früh-Green, G L, Olson, E J, Lupton, J E, Sylva, S P and Kelley, D S. 2008. Abiogenic hydrocarbon production at Lost City hydrothermal field. *Science*, 319: 604–607.
- Pyzik, A J and Sommer, S E. 1981. Sedimentary iron monosulfide: Kinetics and mechanism of formation. *Geochim Cosmochim Acta*, 45: 687–698.
- Rabus, R, Hansen, T A and Widdel, F. 2013. Dissimilatory sulfate- and sulfur-reducing prokaryotes. In, *The Prokaryotes: Prokaryotic Physiology and Biochemistry*, Rosenberg, E, DeLong, E F, Stackebrandt, E, Lory, S and Thompson, F. (Eds.), pp. 309–404.
- Rabus, R, Hansen, T A and Widdel, F. 2013. Dissimilatory sulfate- and sulfur-reducing prokaryotes. *The Prokaryotes: Prokaryotic Physiology and Biochemistry*: 309–404.

- Ragsdale, S W, Pierce, E. 2008. Acetogenesis and the Wood-Ljungdahl pathway of CO<sub>2</sub> fixation. *Biochim Biophys Acta – Proteins and Proteomics*, 1784: 1873-1898.
- Ranjan, S., Todd, Z R, Sutherland, J D and Sasselov, D D. 2018. Sulfidic Anion Concentrations on Early Earth for Surficial Origins-of-Life Chemistry. *Astrobio*, 18: 1023–1040.
- ratios by SIMS: matrix effects for oxygen, carbon and sulfur isotopes in minerals. *Int. J. Mass Spectrom*, 178: 81–112.
- Rawlings, D. E., H. Tributsch, and G. S. Hansford. 1999. Reasons why 'Leptospirillum'-like species rather than *Thiobacillus ferrooxidans* are the dominant iron-oxidizing bacteria in many commercial processes for the biooxidation of pyrite and related ores. *Microbiol* 145: 5–13.
- Rhodes, Frank HT. "Gradualism, punctuated equilibrium and the origin of species." *Nature* 305.5932 (1983): 269-272.
- Riciputi, L R, Paterson, B A and Ripperdan, R L. 1998. Measurement of light stable isotopes
- Rickard, D and Luther, G W. 2007. Chemistry of iron sulfides. *Chem Rev*, 107: 514–562.
- Rimmer, P B and Shorttle, O. 2019. Origin of Life's Building Blocks in Carbon- and Nitrogen-Rich Surface Hydrothermal Vents. *Life*, 9: 12
- Rogers, Karyn L., Jan P. Amend, and Sergio Gurrieri. "Temporal changes in fluid chemistry and energy profiles in the Vulcano island hydrothermal system." *Astrobiology* 7.6 (2007): 905-932.
- Romero, A B and Thiemens, M H. 2003. Mass-independent sulfur isotopic compositions in present-day sulfate aerosols. *J Geophys Res – Atmospheres*, 108: 4524.
- Rosing, M T. 1999. <sup>13</sup>C-Depleted carbon microparticles in >3700-Ma sea-floor sedimentary rocks from West Greenland. *Science*, 283: 674–676.
- Rumble, D., T. C. Hoering, and J. M. Palin. "Preparation of SF<sub>6</sub> for sulfur isotope analysis by laser heating sulfide minerals in the presence of F<sub>2</sub> gas." *Geochimica et Cosmochimica Acta* 57.18 (1993): 4499-4512.
- Russell, M J and Martin, W. 2004. The rocky roots of the acetyl coenzyme-A pathway. *Trends Biochem Sci* 24: 358–363.

- Russell, M J and Nitschke, W. 2017. Methane: Fuel or Exhaust at the Emergence of Life? *Astrobiology*, 17: 1053–1066.
- Russell, M J, Nitschke, W and Branscomb, E. 2013. The inevitable journey to being. *Philos Trans R Soc Lond B Biol Sci* 368, doi:10.1098/rstb.2012.0254.
- Sageman, J, Jørgensen, B B and Greif, O. 1998. Temperature dependence and rates of sulfate reduction in cold sediments of Svalbard, Arctic Ocean. *Geomicrobiol. J.* 15: 85–100.
- Savarino, J, Romero, A, Cole-dai, J, Bekki, S and Thiemens, M H. 2003. UV induced mass-independent fractionations in stratospheric volcanic sulfate. *Geophy Res Lett*, 30: 1–4.
- Scaillet, B, Clemente, B, Evans, B W and Pichavant, M. 1998. Redox control of sulfur degassing in silicic magmas. *J Geophys Res Atmospheres*, 1032: 23937–23950.
- Schauder R, Preuß A, Jetten M and Fuchs G .1988. Oxidative and reductive acetyl CoA/carbon monoxide dehydrogenase pathway in *Desulfobacterium autotrophicum*. 2. Demonstration of the enzymes and comparison of CO dehydrogenase. *Arch Microbiol* 151:84–89.
- Schidlowski M, Eichmann, R and Junge C E. 1975. Precambrian sedimentary carbonates: carbon and oxygen isotope geochemistry and implications for the terrestrial oxygen budget. *Precambrian Res* 2: 1–69.
- Schidlowski M. 1988. A 3,800-million-year isotopic record of life from carbon in sedimentary rocks. *Nature*, 333: 313–318.
- Schidlowski, M, Hayes, J M and Kaplan, I R. 1983. Isotopic inferences of ancient biochemistries: carbon, sulfur, hydrogen and nitrogen. in J.W. Schopf (Ed.), *Earth's Earliest Biosphere: Its Origin and Evolution*, Princeton University Press, New Jersey, pp. 149-186.
- Schidlowski, M. 1982. Content and isotopic composition of reduced carbon in sediments. *In*, Holland, H D and Schidlowski, M (eds.) *Mineral deposition and the evolution of the biosphere*. Dahlem Konferenzen, Berlin: Springer-Verlag. Pp. 103-122.
- Schink B. Energetics of syntrophic cooperation in methanogenic degradation. *Microbio Molec Bio Rev* 61: 262-280.

- Schönheit, P, Buckel, W and Martin, W F. 2016. On the origin of heterotrophy. *Trends Microbiol* 24: 12–25.
- Schoonen, M A A and Barnes, H L. 1991. Reactions forming pyrite and marcasite from solution: I. Nucleation of FeS<sub>2</sub> below 100°C. *Geochim. Cosmochim. Acta*, 55: 1495–1504.
- Schut G J, Boyd, E S, Peters, J W and Adams, M W. 2013. The modular respiratory complexes involved in hydrogen and sulfur metabolism by heterotrophic hyperthermophilic archaea and their evolutionary implications. *FEMS Microbiol Rev.* 37: 182–203.
- Schwieterman, Edward W., et al. "Rethinking CO Antibiosignatures in the Search for Life Beyond the Solar System." *The Astrophysical Journal* 874.1 (2019): 9.
- Segel, I H, Renosto, F and Seubert, PA. 1987. Sulfate-activating enzymes. *Methods in enzymology*. 143. Academic Press, 334–349.
- Shen, Y A, Buick, R and Canfield, D E. 2001. Isotopic evidence for microbial sulphate reduction in the early Archaean era. *Nature*, 410: 77–81.
- Shen, Y N, Farquhar, J, Masterson, A, Kaufman, A J and Buick, R. 2009. Evaluating the role of microbial sulfate reduction in the early Archean using quadruple isotope systematics. *Earth Planet Sci Lett*, 279 :383–391.
- Sim, M S, Ogata, H, Lubitz, W, Adkins, J F, Sessions, A L, Orphan, V J and McGlynn, S. 2019. Role of APS reductase in biogeochemical sulfur isotope fractionation. *Nature Comm*, 10: 1-9.
- Simon, J and Kroneck, P M H. 2013. Microbial sulfite respiration. *Adv Microb Phys.* Vol. 62. Academic Press, pp. 45–117.
- Simon, J and Kroneck, P M H. 2013. Microbial sulfite respiration. *Advances in Microbial Physiology* 62. Academic Press, pp. 45–117.
- Sleep, N H and Bird, D K. 2007. Niches of the pre-photosynthetic biosphere and geologic preservation of Earth's earliest ecology. *Geobiology*, 5: 101–117.
- Smith, Albertus JB, Nicolas J. Beukes, and Jens Gutzmer. "The composition and depositional environments of Mesoarchean iron formations of the West Rand Group of the Witwatersrand Supergroup, South Africa." *Economic Geology* 108.1 (2013): 111-134.

- Sojo, V, Herschy, B, Whicher, A, Camprubí, E and Lane, N. 2016. The origin of life in alkaline hydrothermal vents. *Astrobiology* 16: 181–197.
- Sousa, F L, Preiner, M and Martin, W F. 2018. Native metals, electron bifurcation, and CO<sub>2</sub> reduction in early biochemical evolution. *Curr. Opinion Microbiol*, 43:77–83.
- Stern, Richard A., and Wouter Bleeker. "Age of the world's oldest rocks refined using Canada's SHRIMP: The Acasta Gneiss Complex, Northwest Territories, Canada." *Geoscience Canada* (1998)
- Studel, R. 2003. Inorganic Polysulfides S<sub>n</sub><sup>2-</sup> and Radical Anions S<sub>n</sub><sup>•-</sup>. In, *Topics in Current Chemistry* 231, Elemental Sulfur and Sulfur-rich Compounds II. Berlin, Springer, pp. 127–152.
- Strauss, H. 1993. The sulfur isotopic record of Precambrian sulfates – new data and a critical evaluation of the existing record. *Precamb Res*, 63: 225–246.
- Strauss, H. 1997. The isotopic composition of sedimentary sulfur through time. *Palaeogeog Palaeoclimat Palaeoecol* 132: 97–118.
- Strauss, H. 2003. Sulphur isotopes and the Early Archaean sulphur cycle. *Precamb Res*, 126: 349–361.
- Susanti D and Mukhopadhyay B. 2012. An intertwined evolutionary history of methanogenic archaea and sulfate reduction. *PLoS One*, 7:e45313.
- Takai, K, Gamo, T, Tsunogai, U, Nakayama, N, Hirayama, H, Nealson, K H and Horikoshi, K. 2004. Geochemical and microbiological evidence for a hydrogen-based, hyperthermophilic subsurface lithoautotrophic microbial ecosystem (HyperSLiME) beneath an active deep-sea hydrothermal field. *Extremophiles* 8: 269–282.
- Tashiro, T, Ishida, A, Hori, M, Igisu, M, Koike, M, Méjean, P, Takahata, N, Sano Y and Komiya, T. 2017. Early trace of life from 3.95 Ga sedimentary rocks in Labrador, Canada. *Nature*, 549: 516–518.
- Thamdrup, B, Finster, K, Fossing, H, Hansen, J W and Jørgensen, B B. 1994. Thiosulfate and sulfite distribution in porewater marine sediments related to manganese, iron and sulfur geochemistry. *Geochim Cosmochim Acta* 58: 67–73.

- Thamdrup, B, Finster, K, Hansen, J W and Bak, F. 1993 Bacterial disproportionation of elemental sulfur coupled to chemical-reduction of iron or manganese. *Appl Environ Microbio*, 59: 101–108.
- Thauer, R K, Kaster, A-K, Seedorf, H, Buckel, W and Hedderich, R. 2008. Methanogenic archaea: ecologically relevant differences in energy conservation. *Nat Rev Microbiol* 6: 579-591.
- Thiemens, M H and Lin, M. 2019. Use of isotope effects to understand the present and the past of the atmosphere and climate and track the origin of life. *Angew Chem Int Ed*, 58: 6826–6844.
- Thode, H G, Kleerekoper, H and McElcheran, D. 1951. Isotope fractionation in bacterial fractionation of sulphate. *Research (London)*, 4: 581-582.
- Thode, H G, Macnamara, J and Collins C B. 1949. Natural variations in the isotopic content of sulphur and their significance. *Canad. J. Res. B*, 27: 361–373.
- Thomassot, E, O'Neil, J, Francis, D, Cartigny, P and Wing, B A. 2015. Atmospheric record in the Hadean Eon from multiple sulfur isotope measurements in Nuvvuagittuq Greenstone Belt (Nunavik, Quebec). *Proc Nat Acad Sci USA*, 112: 707–712.
- Thomazo, C, Pinti, D L, Busigny, V, Ader, M, Hashizume, K and Philippot, P. 2009. Biological activity and the Earth's surface evolution: Insights from carbon, sulfur, nitrogen and iron stable isotopes in the rock record. *C. R. Palevol*, 8: 665–678.
- Trolard, F, Génin, J-M R, Abdelmoula, M, Bourrié, G, Humbert, B and Herbillon, A. 1997. Identification of a green rust mineral in a reductomorphic soil by Mossbauer and Raman spectroscopies. *Geochim Cosmochim Acta*, 1: 1107–1111.
- Trudinger, P A, Chambers, L A and Smith, J W. 1985. Low temperature sulphate reduction: Biological vs. abiological. *Canadian J Earth Sci*, 22: 1910–1918.
- Ueda, Akira, and H. Roy Krouse. "Direct conversion of sulphide and sulphate minerals to SO<sub>2</sub> for isotope analyses." *Geochemical Journal* 20.4 (1986): 209-212.
- Ueno, Y, Yamada, K, Yoshida, N, Maruyama, S and Isozaki, Y. 2006. Evidence from fluid inclusions for microbial methanogenesis in the early Archaean era. *Nature* 440: 516–518.



- Urey, H C. 1947. Thermodynamic properties of isotopic substances. *J Chem Soc*, 1947: 562–581.
- Urich, T T, Bandejas, T M, Leal, S S, Rachel, R, Albrecht, T, Zimmermann, P, Scholz, C, Teixeira, M, Gomes, C M and Kletzin, A. 2004. The sulphur oxygenase reductase from *Acidianus ambivalens* is a multimeric protein containing a low-potential mononuclear non-haem iron centre. *Biochem J* 381: 137–146.
- Van Kranendonk, Martin J., et al. "Geological setting of Earth's oldest fossils in the ca. 3.5 Ga Dresser Formation, Pilbara Craton, Western Australia." *Precambrian Research* 167.1-2 (2008): 93-124.
- Van Kranendonk, M. J., et al. "Age, lithology and structural evolution of the c. 3.53 Ga Theespruit Formation in the Tjakastad area, southwestern Barberton Greenstone Belt, South Africa, with implications for Archaean tectonics." *Chemical Geology* 261.1-2 (2009): 115-139.
- Varma, S J, Muchowska, K B, Chatelain, P and Moran, J. 2018. Native iron reduces CO<sub>2</sub> to intermediates and end-products of the acetyl CoA pathway. *Nat Ecol Evol*, 2: 1019–1024.
- Vinyard, David J., et al. "Photosystem II oxygen-evolving complex photoassembly displays an inverse H/D solvent isotope effect under chloride-limiting conditions." *Proceedings of the National Academy of Sciences* 116.38 (2019): 18917-18922.
- Wacey, D, McLoughlin, N, Whithouse, M J and Kilburn, M R. 2010. Two existing sulfur metabolisms in a ca. 3400 Ma sandstone. *Geology*, 38: 1115–1118.
- Ward, L M, Rasmussen, B and Fischer, W W. 2019. Primary productivity was limited by electron donors prior to the advent of oxygenic photosynthesis. *J Geophys Res – Biogeosciences*, 124: 211–226.
- Watanabe, Y, Farquhar, J and Ohmoto, H. 2009. Anomalous fractionations of sulfur isotopes during thermochemical sulfate reduction. *Science*, 324: 370–373.
- Watanabe, Y., Farquhar, J. and Ohmoto, H. 2009. Anomalous fractionations of sulfur isotopes during thermochemical sulfate reduction. *Science* 324: 370–373.

- Watson, E B, Cherniak, D J and Frank, E B. 2009. Retention of biosignatures and mass-independent fractionations in pyrite: Self-diffusion of sulfur. *Geochim Cosmochim Acta*, 73: 4792-4802.
- Weiss, M C. Sousa, F L, Mrnjavac, N, Neukirchen, S, Roettger, M, Nelson-Sathi, S and Martin W F. 2016. The physiology and habitat of the last universal common ancestor. *Nature Microbio*, 1: 16116.
- Weissgerber, T, Sylvester, M, Kröninger, L and Dahl, C. 2014. A comparative quantitative proteomic study identifies new proteins relevant for sulfur oxidation in the purple sulfur bacterium *Allochromatium vinosum*. *Appl Env Microbiol* DOI: 10.1128/AEM.04182-13
- Whitehall, A R and Ono, S. 2012. Excitation band dependence of sulfur isotope mass-independent fractionation during photochemistry of sulfur dioxide using broadband light sources. *Geochim Cosmochim Acta*, 94: 238–253.
- Whitehouse, M J, Dunkley, D J, Kusiak, M A and Wilde, S A. 2019. On the true antiquity of Eoarchean chemofossils – assessing the claim for Earth’s oldest biogenic graphite in the Saglek Block of Labrador. *Precamb Res*, 323:70–81.
- Whitehouse, M J, Myers, J M and Fedo, C M. 2009. The Akilia Controversy: field, structural and geochronological evidence questions interpretations of > 3.8 Ga life in SW Greenland. *J Geol Soc London*, 166: 335–348.
- Wille, Martin, et al. "Mo–Cr isotope evidence for a reducing Archean atmosphere in 3.46–2.76 Ga black shales from the Pilbara, Western Australia." *Chemical Geology* 340 (2013): 68-76.
- Whiticar, M J and Faber, E. 1986. Methane oxidation in sediment and water column environments - Isotope evidence. *Org Geochem* 10: 759–768.
- Widdel, F and Pfennig, N. 1981. Studies on dissimilatory sulfate-reducing bacteria that decompose fatty acids. *Arch Microbiol*, 129: 395–400.
- Xiong, J. 2007. Photosynthesis: what color was its origin? *Genome Biol*, 7: 245.
- Xu, Y, Schoonen, M A A, Cunningham, K M and Ball, J W. 1998. Sulfur geochemistry of hydrothermal waters in Yellowstone National Park- I. The origin of thiosulfate in hot spring waters. *Geochim Cosmochim Acta*, 62: 3729–3743.

- Young, E D, Galy, A and Nagahara, H. 2002. Kinetic and equilibrium mass-dependent isotope fractionation laws in nature and their geochemical and cosmochemical significance. *Geochimica Et Cosmochimica Acta*, 66: 1095–1104.
- Zawaski, M, Kelly, N M, Orlandini, O M, Allwood, A C, Nichols, C I O and Mojzsis, S J. 2020. Reappraisal of purported ca. 3.7 Ga stromatolites from the Isua Supracrustal Belt (West Greenland) from detailed chemical and structural analysis. *Earth Planet Sci Lett*, in revisions.
- Zhang, Lianchang, et al. "Formation age and tectonic setting of the Shirengou Neoproterozoic banded iron deposit in eastern Hebei Province: constraints from geochemistry and SIMS zircon U–Pb dating." *Precambrian Research* 222 (2012): 325-338.
- Zhelezinskaia, I, Kaufman, A J, Farquhar, J and Cliff, J. 2014. Large sulfur isotope fractionations associated with Neoproterozoic microbial sulfate reduction. *Science* 346: 742–744.
- Zopfi, J, Ferdelman, T G and Fossing, H. 2004. Distribution and fate of sulfur intermediates—sulfite, tetrathionate, thiosulfate, and elemental sulfur in marine sediments, *In* Amend, JP, Edwards, K J and Lyons, T W, eds., *Sulfur biogeochemistry—Past and present*: Boulder, Colorado, Geological Society of America Special Paper 379, p. 97–116.

**Supplementary Info:**

Data and references for figure 2 and 7 on [github](#).